Corresponding Editor:

Stephanie C. Herring, PhD
NOAA National Climatic Data Center
325 Broadway, E/CC23, Rm 1B-131
Boulder, CO, 80305-3328
E-mail: stephanie.herring@noaa.gov

Cover credits:

Front: The final wave of rain storms make their way through Boulder, Colorado, bringing another day of flooding to the already rain swollen area, 15 September 2013. Image by ©Ed Endicott/Demotix/Corbis.

Back: The city of Boulder, Colorado, experienced substantial flooding for four days that have lasting effects, 18 September 2013. Image by ©Anna M Weaver/Demotix/Corbis.

HOW TO CITE THIS DOCUMENT

Citing the complete report:

Herring, S. C., M. P. Hoerling, T. C. Peterson, and P. A. Stott, Eds., 2014: Explaining Extreme Events of 2013 from a Climate Perspective. *Bull. Amer. Meteor. Soc.*, **95** (9), S1–S96.

Citing a section (example):

Hoerling, M., and Coauthors, 2014: Northeast Colorado extreme rains interpreted in a climate change context [in "Explaining Extremes of 2013 from a Climate Perspective"]. *Bull. Amer. Meteor. Soc.*, **95** (9), S15–S18.

EDITORIAL AND PRODUCTION TEAM

Riddle, Deborah B., Lead Graphics Production, NOAA/NESDIS National Climatic Data Center, Asheville, NC
Veasey, Sara W., Graphics Team Lead, NOAA/NESDIS National Climatic Data Center, Asheville, NC
Griffin, Jessica, Graphics Support, CICS-NC, Asheville, NC
Love-Brotak, S. Elizabeth, Graphics Support, NOAA/NESDIS National Climatic Data Center, Asheville, NC
Misch, Deborah J., Graphics Support, JPS, Inc., NOAA/NESDIS National Climatic Data Center, Asheville, NC
Osborne, Susan, Copy Editor, JPS, Inc., NOAA/NESDIS National Climatic Data Center, Asheville, NC
Sprain, Mara, Editorial Support, LAC Group, NOAA/NESDIS National Climatic Data Center, Asheville, NC
Young, Teresa, Graphics Support, ERT/STG, Inc., NOAA/NESDIS National Climatic Data Center, Asheville, NC

shift towards a reduction in the magnitude of extremes in MD runs with a multimodel mean decrease of around one-third (Fig. 7.2). Likewise, while two models showed a nonsignificant increase for a 90th percentile early autumn maximum daily SWE, the MD runs primarily tended toward reduced magnitude (mean decrease of 20%) relative to PI runs. However, the changes for both metrics were only significant for a single model and were not considered a robust change. These results largely mirrored projected changes in early autumn SWE that showed intermodel agreement of reduced SWE relative to PI runs (mean decrease of 35%). By contrast, simulated differences in early autumn maximum daily precipitation and the 90th percentile early autumn daily precipitation showed nominal and mixed changes. Increased PW in MD runs relative to PI was found consistently across the study area and was consistent with overall increases in temperature and potential water holding capacity scaling with the Clausius–Clapeyron relationship.

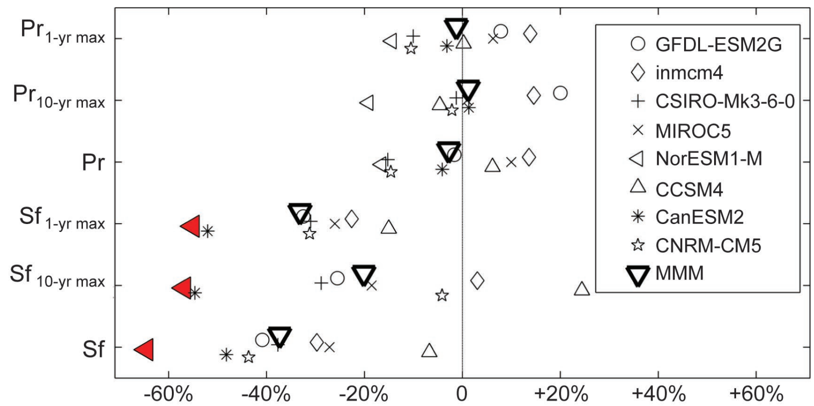

Fig. 7.2. Intramodel differences in the percent change in precipitation (Pr) and snowfall (Sf) between MD and PI in western South Dakota over a 30-day period centered on October 4. Differences are shown for annual extreme (1-yr max), 1-in-10 year annual extreme (10-yr max), and overall means. Statistically significant differences are denoted by red triangles; open triangles denote the eight-model average. A list of the models used is provided in Supplementary Table S7.1. Increased PW in MD runs relative to PI was found consistently across the study area and was consistent with overall increases in temperature and potential water holding capacity scaling with the Clausius–Clapeyron relationship. These findings also held for differences in early autumn maximum series of PW, with a multimodel increase of around 7% for the study area (not shown).

Conclusions. The record-setting early season blizzard of October 2013 had significant impact on the agriculture, infrastructure, and economy of western SD. This event was associated with highly anomalous (95th to 99th percentile) atmospheric water vapor for early autumn and anomalous, but not unprecedented, 500-hPa heights for any time of year.

While several climate models are consistent with the observations in showing an increase in PW, there is no apparent model agreement regarding changes in extreme precipitation or snowfall in the early autumn season for western SD under modern conditions relative to preindustrial conditions.

8. MULTIMODEL ASSESSMENT OF EXTREME ANNUAL-MEAN WARM ANOMALIES DURING 2013 OVER REGIONS OF AUSTRALIA AND THE WESTERN TROPICAL PACIFIC

Thomas R. Knutson, Fanrong Zeng, and Andrew T. Wittenberg

CMIP5 simulations suggest that the extremely warm year observed over Australia and the far western Pacific during 2013 was largely attributable to human forcing of the climate system.

Introduction. A global survey of surface temperature anomalies occurring during 2013 (Fig. 8.1a; Supplementary Fig. S8.1) in the HadCRUT4 observations (Morice et al. 2012) reveals pronounced warm annual and seasonal mean anomalies. Two regions with prominent record or near-record annual mean warm anomalies include large regions of Australia and a region in the far western tropical Pacific encompassing the Philippines and part of the Maritime Continent (Fig. 8.1b). The 2013 anomalies appear particularly extreme during austral fall and winter (MAM, JJA) in Australia and during MAM in the far western Pacific (Supplementary Fig. S8.1). Temperatures in these two regions are further assessed in this report for the causes of this extreme warmth. Twenty-three All-Forcing (anthropogenic plus natural) models and control runs and 10 Natural-Forcing models were used from the Coupled Model Intercomparison Project phase 5 (CMIP5; Taylor et al. 2012). See Knutson et al. (2013a,b) for background on our methodology and a global assessment of low-frequency variability and trends.

Global occurrence rates of record or near-record annual mean surface temperatures. Figure 8.1c,d shows the fraction of available global area with record or near-record (ranked in the top/bottom three with at least 100 years of record) annual mean positive or negative anomalies. In 2013, the fraction of area with record or near-record annual anomalies was very skewed toward warm occurrences, with 10.4% of the analyzed area having annual mean warmth that was first, second, or third highest on record, compared with 0% coverage of record or near-record cold. This continues a feature seen in recent decades, with similar rates for positive extreme occurrences since about 2000 and very little analyzed area with annual mean near-record negative temperature anomalies since about 1990. The large occurrence rates of record or near-record annual mean temperature anomalies is high in the early parts of the record as an artifact of the short record lengths, so the focus should be on the latter parts of the record. Figure 8.1d shows the annual rates using the full record to assess each year, including the early years, and shows the preference for cold mean annual extremes prior to about 1920 and the increasing preference for warm annual mean extremes since about 1990. Although global mean temperature has experienced a "hiatus" or pause since around 2000 (e.g., Fyfe et al. 2013), this pause has occurred at high overall temperature levels relative to the late 1800s, resulting in a much more common occurrence of regional seasonal and annual warm temperature records (or near records) around the globe compared to cold records (Fig. 8.1c,d). Seneviratne

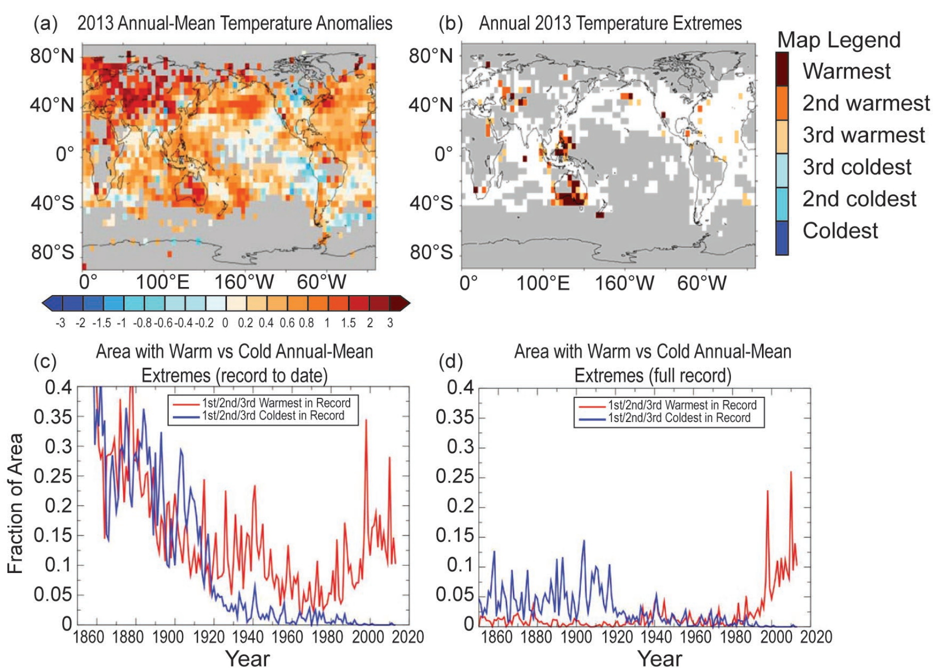

Fig. 8.1. (a) Annual-mean surface air temperature anomalies (°C) for 2013 (1961–1990 base period) from the HadCRUT4 data set. (b) Colors identify grid boxes with annual-mean warm anomalies that rank first (dark red), second (orange-red), or third (yellow-orange) in the available observed record. Gray areas did not have sufficiently long records, defined here as containing at least 100 available annual means, with a seasonal mean requiring at least one of three months to be available, and an annual mean requiring at least three of four seasons to be available. (c) Fraction of available global area by year where the given year's annual mean anomalies for that area rank in the top three highest (red curve) or lowest (blue curve) in the available record to that date. Available area restricted to those regions having at least 100 years of available data through 2013. (d) As in (c) but comparing each year's annual anomalies to the entire record through 2013 (i.e., at least 100 years of data) for that gridpoint.

et al. (2014) have similarly found that there has been a continued increase in warm daily temperature extremes over global land regions during the "hiatus" period.

Is there a significant long-term anthropogenic warming trend in the Australian and far western Pacific regions? Annual-mean temperature anomaly time series extending back to the late 1800s for Australia and western tropical Pacific regions are shown in Fig. 8.2a,b. Both observed series (black curves) show a pronounced long-term warming, which has been more rapid since ~1970. This general behavior is well captured by the CMIP5 All-Forcing ensemble (red curves), though not by the Natural-Forcing ensemble (blue curves). The western tropical Pacific region has warmed slightly less than the global mean since the 1881–1920 base period, while the Australia region warming has been roughly comparable to that of the global mean (e.g., green curve in Fig. 8.2b).

To assess the causes of the observed long-term warming, we use a "sliding trend" analysis (Knutson et al. 2013a,b), incorporating multimodel samples from CMIP5 control runs and ensemble mean forced trends (Fig. 8.2c,d). The plots compare linear trends in the observations (black lines) with models, for trends ending in 2013 and beginning with a range of start years from the late 1800s to very recent. The pink region represents the "All-Forcing hypothesis"—the 5th–95th percentile range of trends from the All-Forcing runs. It is constructed as an ensemble distribution, aggregating the distributions of trends from the 23 individual CMIP5 models. Each model's ensemble-mean All-Forcing trend is combined with randomly sampled internally generated trends from that model's control run. These 23 distributions are aggregated to form the full distribution whose 5th–95th percentile range is depicted by the pink region, which thus reflects uncertainty in both the forced response and the influence of internal variability. The alternative "Internal-Variability-Only hypothesis" is shown by the green region on the plot. For comparison, Supplementary Fig. S8.2 shows an "All-Forcing hypothesis" versus a "Natural Forcing-Only" hypothesis version of the "sliding trend" analysis, in this case, for trends ending in 2012 (as a sensitivity test) and based on a 10-model subset of CMIP5 models with available Natural-Forcing runs through 2012.

The trend assessments in Fig. 8.2c,d and Supplementary Fig. S8.2 show that in both focus regions the observed long-term warming is generally detectable (outside the green band, i.e., significantly larger than simulated internal or natural climate variability), at least for trends beginning earlier than the 1970s. Moreover, the observed trends are generally consistent with the "All-Forcing" hypothesis (pink region) for trends beginning in these periods. Using the CMIP5 models' simulated variability and responses to natural forcings to estimate real-world natural variability (see internal variability assessments in Knutson et al. 2013a), we conclude that the long-term observed trends in both regions are very likely inconsistent with natural variability but generally consistent with anthropogenic and natural forcing combined. Therefore, the model results suggest that the long-term observed warming in both regions is very likely attributable in part to anthropogenic forcing.

To what extent are the 2013 extreme annual mean temperatures attributable to anthropogenic forcing? We next assess the 2013 annual mean temperature anomalies in the two regions using All-Forcing and Natural-Forcing scenarios (Fig. 8.2e,f). For the All-Forcing runs (red), the CMIP5 historical runs are extended as necessary through 2013 using the RCP4.5 forcing scenario. However, the Natural-Forcing runs (blue) cannot be extended in this manner, and so the Natural-Forcing ensemble response for 2013 is estimated by using the 2012 ensemble mean of the models along with high and low sensitivity tests (Fig. 8.2a,b; see Supplemental Material). Using the 2012 Natural Forcing estimate, the observed 2013 anomalies (compared to a baseline for 1881–1920) are well outside the range of CMIP5 model-estimated natural climate variability for both regions (Fig. 8.2e,f). We use 1881–1920 as a reference value for the 2013 anomaly, as we are attempting to estimate anthropogenic contributions and so have chosen a relatively early baseline period to be closer to preindustrial conditions. Further discussion of the baseline period and observational uncertainties is contained in the Supplemental Material. According to our analysis, the Australia region 2013 anomaly of 1.72°C had contributions of 0.81°C (anthropogenic forcing), 0.23°C (natural forcing), and 0.68°C (natural internal variability). The observed 1.72°C anomaly was at the 99.3 percentile of the CMIP5 All-Forcing distribution and was much larger than the ensemble mean of the All-Forcing distribution (1.04°C). This suggests that either internal variability played a significant role (in addition to external forcing) in producing the 2013 anomaly (estimated as 0.68°C), or the net climate forcing or the response to climate forcing in the CMIP5 models could be too

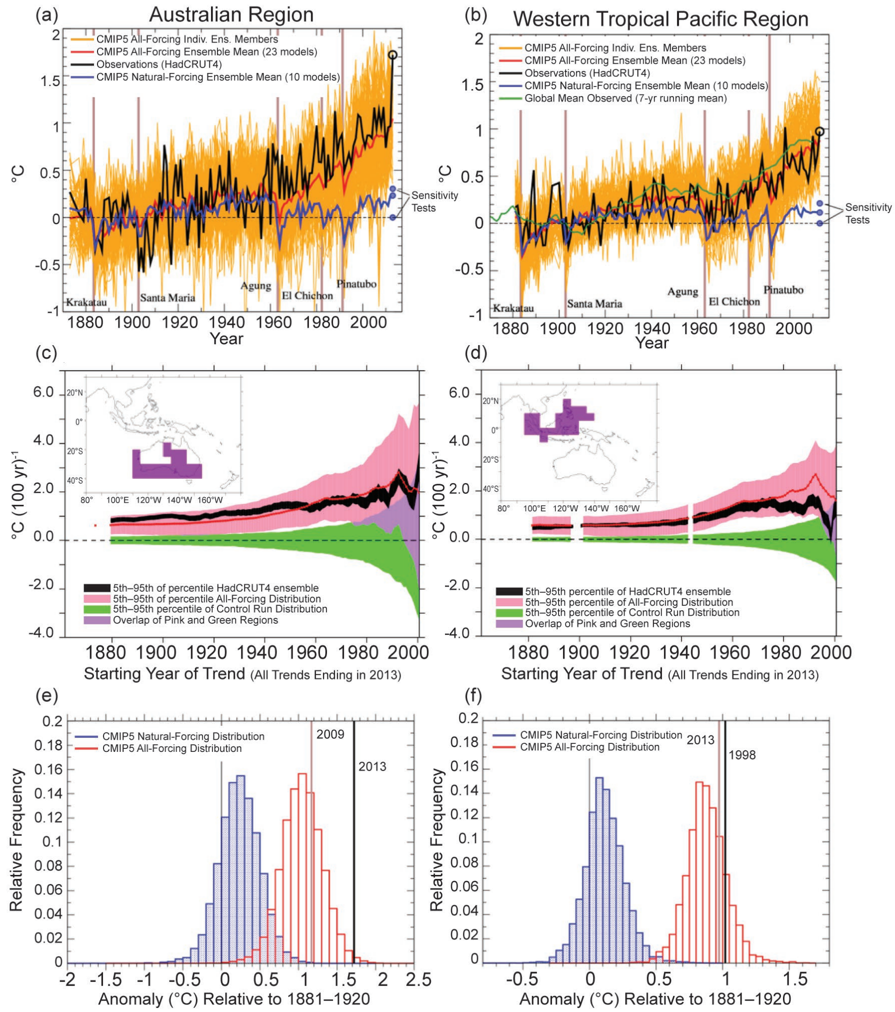

Fig. 8.2. (a,b) Time series of annual averaged surface temperature anomalies (°C) averaged over regions of (a) Australia, left column, and (b) the far western tropical Pacific, right column . The black curves depict the observed (HadCRUT4) anomalies; the dark red (dark blue) curves depict the multi-model ensemble anomalies from the CMIP5 All-Forcing (Natural Forcing-only) runs, with each of the 23 (10) available models weighted equally; the orange curves are individual All-Forcing ensemble members. The green curve in (b) is the 7-yr running mean observed global mean temperature anomaly. The three blue circles labelled "Sensitivity Tests" depict low, medium, and high estimates of the Natural Forcing-only response for 2013 (see Supplemental Material). The All-Forcing simulations for these regions included both anthropogenic and natural forcings from about 1860 to the present, with data from RCP4.5 runs used to extend the time series through 2013 where necessary. Only 10 models had Natural Forcing runs available to us through 2012. All time series shown are adjusted to have zero mean over the period 1881–1920. (c,d) Trends [°C (100 yr^{-1})] in the area-averaged annual-mean surface temperature series in (a,b) as a function of starting year, with all trends ending in 2013. The black curves show trends from observations (HadCRUT4), with the black shading depicting the 5th–95th percentile range for the 100-member HadCRUT4 observed ensemble (Morice et al. 2012), giving one indication of the observational uncertainty in these results. The red curves show the inter-model mean of ensemble mean trends from the 23-member CMIP5 All-Forcing ensemble. The pink region represents the 'All Forcing' hypothesis—the 5th–95th percentile range of trends from the All-Forcing runs. The green-shaded region shows the 5th to 95th percentile range of the alternative "Internal Variability Only" hypothesis estimated from the pre-industrial control runs. Purple shading indicates where the pink- and green-shaded regions overlap. The white spaces in the curves denote years where the initial "start year" was missing due to inadequate spatial or temporal coverage. Temporal coverage was assessed as in Fig. 8.1, and the spatial coverage was assessed for each year by requiring at least 33% non-missing annual means for the region. (e,f) Distribution of annual mean anomalies in the CMIP5 Natural Forcing-only runs (blue) and for the All Forcing runs (red) for 2013. The observed temperature anomalies for 2013 are depicted as dark black vertical lines, with anomalies for another recent similarly extreme year shown by the gray vertical lines.

weak. Since an anomaly as large as observed was also outside the estimated range of the natural variability (natural forcing plus internal variability) distribution from the CMIP5 models, our analysis shows that the CMIP5 modeled fraction (or percent) of risk of the event that is attributable to anthropogenic forcing is essentially 100%. The second highest anomaly in the Australia region series (1.17°C in 2009) occurs very rarely if at all in the modeled Natural-Forcing distribution, depending on assumptions on the 2012 natural forcing response (Supplementary Table S8.1). We again conclude that the modeled fraction of risk attributable to anthropogenic forcing is near 100% for this alternative threshold value.

Lewis and Karoly (2013) performed a similar analysis on the full Australia region for summer 2013 (December 2012–February 2013). They find a significant anthropogenic contribution to extreme warmth, with about a seven-fold increase in risk of an event like 2013 for an RCP8.5 scenario centered on the year 2013 (2006–20). The increase in risk that we find is even higher than their estimate, presumably because we analyze only that subset of the Australian region having the most unusual 2013 temperatures and we assess annual means rather than summer mean temperatures. Both of these analysis choices would tend to enhance the signal-to-noise ratio for an anthropogenic warming signal (or relative risk); on the other hand, by analyzing the summer season, Lewis and Karoly (2013) were focused on the season with presumably the maximum heat-stress impact. Our findings are also generally consistent with those of two similar analyses of Australian 2013 annual temperature ("The role of anthropogenic forcing in the record 2013 Australia-wide annual and spring temperatures" and "Climate change turns Australia's 2013 big dry into a year of record-breaking heat" in this report).

For the western tropical Pacific region, the 2013 annual mean anomaly was 0.97°C, or slightly less than the 1998 anomaly of 1.02°C. The estimated contributions to the 2013 anomaly, based on the CMIP5 models, were 0.76°C (anthropogenic forcing), 0.11°C (natural forcing), and 0.09°C (natural internal variability). Both of these observed anomalies (relative to an 1881–1920 baseline) are outside of, or very rarely occurring in, our estimated distribution of natural variability. Thus, the modeled fraction of event risk attributable to anthropogenic forcing is close to 100%. The 2013 anomaly is at the 75.8 percentile of the All-Forcing distribution, indicating either a likely role for natural variability as estimated above or perhaps an underestimated forcing response in this region.

A simple variance consistency test was also done (Supplemental Material) to assess the adequacy of the control runs' internal variability as an estimate of the internal variability of the actual climate system. The latter was estimated by subtracting the CMIP5 models' ensemble-mean All-Forcing response from the observed temperature series. For the Australia region, the residual variability so derived agrees well with the model control run ensemble. For the far western Pacific region, the standard deviation of the observed residual variability is about 16% higher than the control run ensemble, but adjusting the model control run variability upward by over 20% does not impact the main conclusions of our study. Similarly, our attribution conclusions remain robust in light of our assessment of the impact of baseline reference period and other observational uncertainties and related issues as discussed in the Supplemental Material.

Summary. Seasonal and annual temperature anomalies around the globe were highly skewed toward positive (warm) extremes in 2013, as in the recent few decades. Although global warming has been described as "pausing" since 2000, global temperatures remain at anomalously high levels, and warm annual and seasonal temperature extremes continue to far outpace the occurrence of cold annual extremes. Two examples of regions with extreme (record or near-record) annual warmth during 2013 include much of Australia and a region of the far western tropical Pacific. In both regions, a contribution of anthropogenic forcing to an observed long-term warming trend was detected. The annual mean anomalies for 2013 were either completely outside of, or extremely rare in, the distributions of modeled natural variability. Thus, the fraction of risk of these extreme events attributable to anthropogenic forcing was 100% or close to 100%, according to the CMIP5 models. These results reinforce the notion of a potentially high signal-to-noise ratio for anthropogenic warming signals for seasonal and annual anomalies—even at the subcontinental scale in some cases. They further suggest that even if the global warming "hiatus" continues, further extreme (record or near-record) seasonal or annual mean warm anomalies at the regional scale can be anticipated, though the particular regions with such extremes change from year to year (e.g., comparing the present study with our 2012 analysis, Knutson et al. 2013b).

SUPPLEMENT

EXPLAINING EXTREME EVENTS OF 2013 FROM A CLIMATE PERSPECTIVE

Editors
Stephanie C. Herring, Martin P. Hoerling, Thomas C. Peterson, Peter A. Stott,

Special Supplement to the
Bulletin of the American Meteorological Society
Vol. 95, No. 9, September 2014

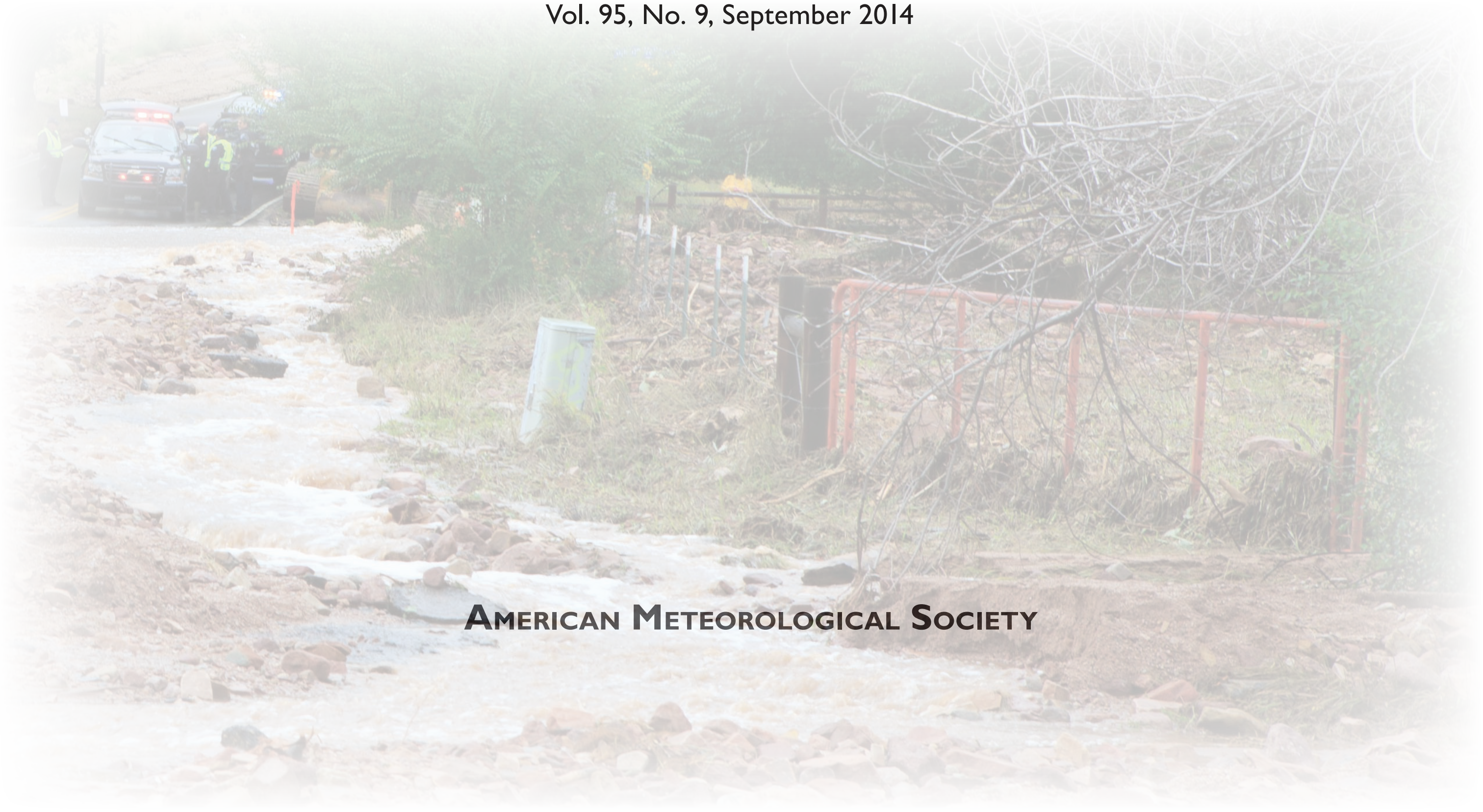

AMERICAN METEOROLOGICAL SOCIETY

S8. MULTIMODEL ASSESSMENT OF EXTREME ANNUAL-MEAN WARM ANOMALIES DURING 2013 OVER REGIONS OF AUSTRALIA AND THE WESTERN TROPICAL PACIFIC

Thomas R. Knutson, Fanrong Zeng, and Andrew Wittenberg

We present here several auxiliary analyzes and figures relevant to our study, which were not possible to include in the main report due to space limits. In Fig. S8.1, we show for reference the seasonal mean anomaly maps and seasonal-mean extreme occurrence maps for temperature, which are analogous to Fig. 8.1 in the main text but for the individual seasons. We also present "sliding trend" analyzes like those in Fig. 8.2 in the main report (c,d) but comparing 10-model Natural Forcing ensembles with 10-model All-Forcing ensemble subsets of the CMIP5 models. We describe some background on our method and rationale for estimating a Natural-Forcing-only ensemble mean model response for 2013, and the sensitivity of our results to this estimate. We assess the adequacy of simulated internal climate variability in the model for the focus regions in our study. Finally, we assess certain observational issues.

'Sliding trend' analysis of Natural Forcing vs. All-Forcing Ensemble. In Fig. S8.2 we present 'sliding trend' analysis of trends of varying lengths, all ending in 2012, for the Australian and far western tropical Pacific regions. These analysis are similar to those in Fig. 8.2 in the main report, but compare the All-Forcing trend distributions from a 10-model subset of the CMIP5 models to the Natural-Forcing trend distributions from the same 10 models. The trend analysis are done through 2012 instead of 2013 (as in the main text) because the Natural Forcing runs generally ended in 2012 and we could also test the sensitivity of our trend analysis to leaving out the highly anomalous 2013 values for the observations.

The results show that for all start dates up until about the late 1970s, the trends (to 2012) in the two regions are detectable compared to the multi-model Natural Forcing trend distributions (i.e., outside of the blue envelope). The trends in the Australia region are consistent with the All-Forcing 10-member ensemble (i.e., within the pink envelope) for virtually all start dates examined up to 2000. The trends for the far western Pacific region are consistent with the All-Forcing 10-member ensemble for start dates up to about the late 1970s.

Thus for most start dates beginning in the late 1800s and extending until at least as late as the late 1970s, the CMIP5 model simulations indicate that there is a detectable anthropogenic influence on temperature trends to 2012 in these two regions, according to our testing methodology.

Estimating the Natural-Forcing-only response for 2013. Since the CMIP5 models typically ended their Natural-Forcing runs between 2005 and 2012, we did not have a readily available 23-model estimate of the Natural Forcing ensemble mean response for 2013. However, 10 models had Natural Forcing runs available through 2012. Inspection of the Natural Forcing ensemble time series from those 10 models, in Fig. 8.2 a,b in the main report, suggests that an approximate Natural Forcing ensemble mean component for 2013 would be to reuse the value simulated for 2012 ("Mid Natural"). As sensitivity tests, we also performed our relative risk and fraction of attributable risk calculations assuming a "Low Natural" case of zero Natural Forcing contribution and a "High Natural" case using the maximum of the ensemble mean Natural Forcing response occurring at any point in the time series from around 1880 to 2012 as the estimate for 2013. A "Low Natural" (and not conservative) estimate is equivalent in this case to comparing the observed 2013 anomaly (relative to 1881–1920 baseline) against model control run variability alone. The various estimates used are shown as blue circles on Fig. 8.2a,b in the main report and listed in the first column of Table S8.1.

The results in Table S8.1 suggest that for all cases examined and for both regions examined, essentially all of the risk of the 2013 events is attributable to anthropogenic forcing, since anomalies as large as those observed in 2013 are either completely outside of the modeled distribution for the Natural Forcing only scenario or are an extremely rare event within that distribution. The analysis is repeated for a threshold temperature anomaly based on an alternative year (1998 for the western tropical Pacific region, which was slightly warmer than 2013, and 2009 for the Australia region, which was essentially tied for second-ranked year but substantially below 2013's anomaly in magnitude). The results (Table S8.1) are robust in suggesting that essentially all of the risk of warm anomalies the size of those during these years is attributable to anthropogenic forcing.

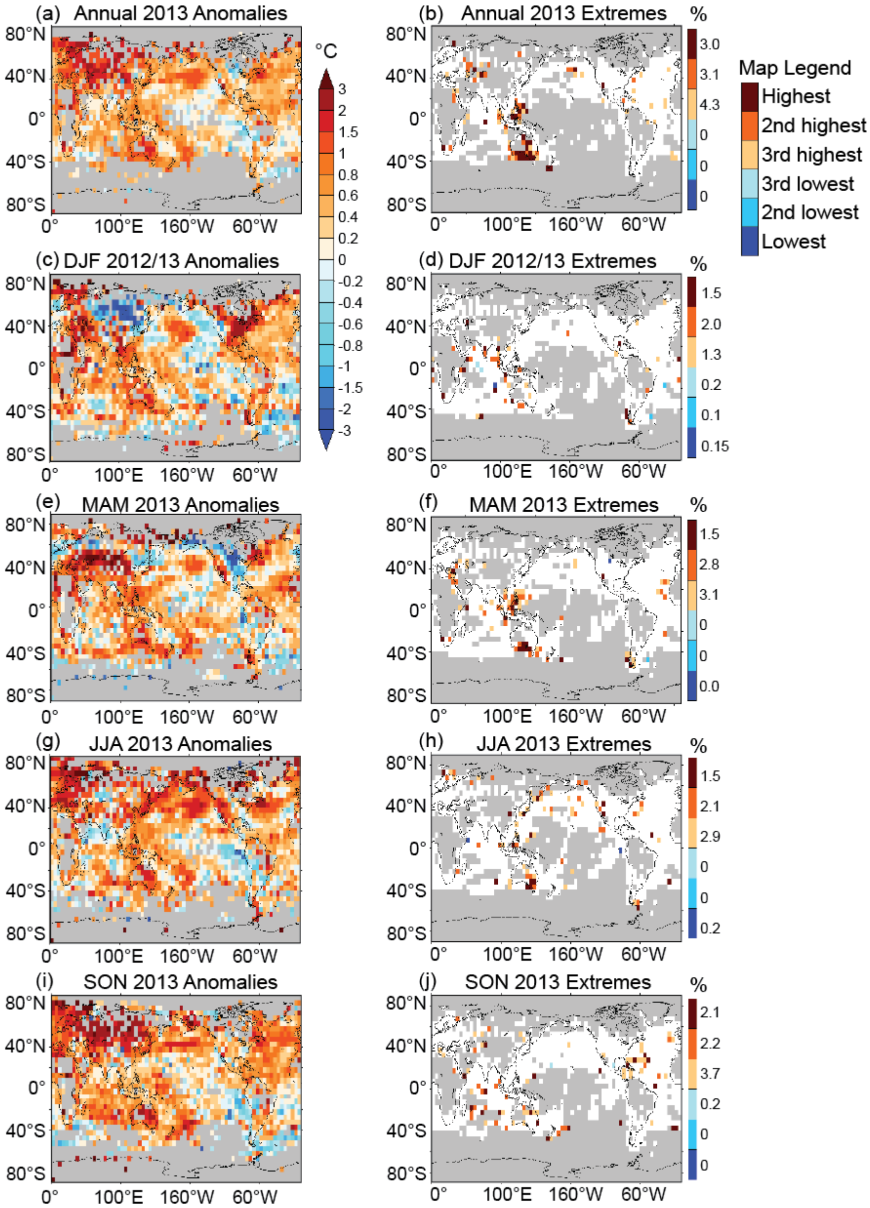

Fig. S8.1. Left column: Annual (a) or seasonal (c,e,g,i) mean surface air temperature anomalies (°C) for 2013 (1961–90 base period) from the HadCRUT4 data set. The seasons are DJF (December 2012–February 2013); MAM (March–May); JJA (June–August); and SON (September–November). Right column: Colors identify grid boxes with annual (b) or seasonal (d,f,h,j) mean warm anomalies that rank 1st (dark red), 2nd (orange-red), or 3rd (yellow-orange) in the available observed record. Gray areas did not have sufficiently long records, defined here as containing at least 100 available annual or seasonal means, with a seasonal mean requiring at least one of three months to be available, and an annual mean requiring at least three of four seasons to be available. The percent values (right side of figures in right column) denote the percent of analyzed area for each category.

Variance consistency test and robustness of findings to standard deviation adjustment. We evaluated the models' control run interannual variability for the two focus regions for consistency with the internal variability estimated from the observations. The latter was estimated by subtracting the intermodel mean ensemble mean All-Forcing time series from the observations, to produce an estimate of the unforced observed residual. The standard deviation, σ, of this "observed" residual for the Australia region is 0.272°C for observations com-

Table S8.1. Estimates of observed and modeled temperature anomaly characteristics for 2013 and an alternative similar year (e.g., 1st or 2nd highest) for the two focus regions. See text for description of cases and the column entries. Anomalies for 2013 are relative to a baseline of 1881–1920. "Inf." indicates cases where the observed anomaly is completely outside of the simulated distribution, so that the relative risk ratio is undefined.

Region/Case (Natural Forcing Estimate in °C)	Observed Anomaly °C for 2013 or Alt. yr.	Observed Percentile in Natural Dist. [%] (2013; Alt. yr)	Observed Percentile in All-Forcing Dist. [%] (2013; Alt. yr.)	Fraction of Attributable Risk (2013; Alt. yr)	Relative Risk (2013; Alt yr)
Australia Region *(unadjusted)*					
High Natural (0.304)	1.72; 1.17	Inf.; 99.9	99.3; 68.4	1.00; 1.00	Inf.; 376
Medium Natural (0.232)		Inf.; 100.0.	99.3; 68.4	1.00; 1.00	Inf.; 1330.
Low Natural (0.000)		Inf.; Inf.	99.3; 68.4	1.00; 1.00	Inf.; Inf.
Western Tropical Pacific Region *(unadjusted)*					
High Natural (0.212)	0.97; 1.02	100.0; Inf	75.8; 84.1	1.00; 1.00	5130; Inf.
Medium Natural (0.115)		Inf.; Inf.	75.8; 84.1	1.00; 1.00	Inf.; Inf.
Low Natural (0.000)		Inf.; Inf.	75.8; 84.1	1.00; 1.00	Inf.; Inf.
Western Tropical Pacific Region *(adjusted std dev)*					
High Natural (0.212)	0.97; 1.02	99.9; 100.0	72.1; 79.9	1.00; 1.00	227; 582
Medium Natural (0.118)		100.0; 100.0	72.1; 79.9	1.00; 1.00	1370; 2790
Low Natural (0.000)		Inf.; Inf.	72.1; 79.9	1.00; 1.00	Inf; Inf.

pared with 0.266°C for the multimodel sample of control runs, indicating good agreement. The standard deviation of the full observed time series is 0.421°C. Thus, while the observed 2013 anomaly of 1.72°C is about a 4σ event in the observed record (σ = 0.421°C), it represents an estimated 6σ event compared to modeled internal variability.

For the far western tropical Pacific region, the estimated interannual standard deviation from the observed residuals is 0.172°C or 16% higher than the interannual standard deviation of the control runs. The observed 2013 anomaly of 0.97°C is almost a 4σ event in the total observed distribution of annual temperatures but a 6σ event compared to the estimated internal variability. As a sensitivity test, we scaled the western Pacific region modeled (control run) anomalies up by a factor of 1.22, which slightly exceeds the amount necessary to adjust for the estimated low variability bias. The results shown in Table S8.1 (adjusted) do not change the basic conclusion that according to the models, the 2013 annual warm anomaly in this region is essentially entirely attributable to anthropogenic forcing in terms of its risk of occurrence.

Assessment of observational uncertainties. Here we consider some observational uncertainty issues. Our sliding trend analyses (e.g., Fig. 8.2c,d in the main report; Fig. S8.2) show via the black shading the 5th–95th percentile range of trends obtained using the 100-member HadCRUT4 observed ensemble (Morice et al. 2012), giving one indication of the observational uncertainty in these trend results. These indicate that our basic findings are robust to this estimate of observational uncertainty. A related issue is whether our results could depend on the use of the HadCRUT4 data, as opposed to an alternative dataset from the Australian Bureau of Meteorology (BOM) that is available for the relatively well-sampled period 1910–2013. We downloaded an all-Australia index of temperature anomalies from the BOM data at: http://www.bom.gov.au/climate/change/index.shtml#tabs=Tracker&tracker=timeseries.

First, we compare the BOM time series cited above (1910–2013) to the HadCRUT4 data averaged over roughly the same Australia region (not the identical region because the HadCRUT4 is available on a 5° x 5° grid). Figure S8.3 shows a comparison of the seven-year running mean time series derived from the BOM and HadCRUT4 data (reference period 1961–90). This shows that the anomalies in these two datasets are very similar when averaged over the Australian region as a whole. Our main analysis focuses on a sub-region of Australia based on those areas with extreme annual means as identified in Fig. 8.1 in the main report, and for this, we use the HadCRUT4 data, which seems appropriate based on the above comparison.

Another observational issue is the use of different reference periods for estimating the magnitude of the 2013 anomaly relative to preindustrial levels. In general, we would prefer to use as early a reference period as is practical, since earlier periods are closer to preindustrial conditions and we are trying to estimate the anthropogenically forced departure from such conditions. We find, using the HadCRUT4 data averaged over the Australia sub-region in our study, that the anomaly for the available years in 1881–1920 is about 0.2°C lower than that for 1910–49. This difference is much smaller than the 2013 anomaly of 1.72°C. Even adjusting the 2013 anomaly down by 0.2°C (i.e., using the years 1910–49 as the base period), the resulting anomaly for 2013 (1.52°C) remains outside of the range of anomalies in the Natural Forcing distribution shown in Fig. 8.2e in the main report. In addition, the Natural Forcing response (for 2013, if assumed to be equivalent to that simulated for 2012) is about 0.1°C smaller using the 1910–49 base period than using the 1881–1920 base period (since the 1881–1920 period featured cooler temperature in the Natural Forcing runs). Taking this adjustment into account implies that the required adjustments for the observations versus the Natural Forcing distribution is a net reduction in their separation by only about 0.1°C. Again, we conclude that the observed anomaly is not simulated in the large multimodel sample of annual means for 2013 Natural Forcing conditions. In short, our finding that the 2013 observed anomaly is outside of the range of model simulated natural variability

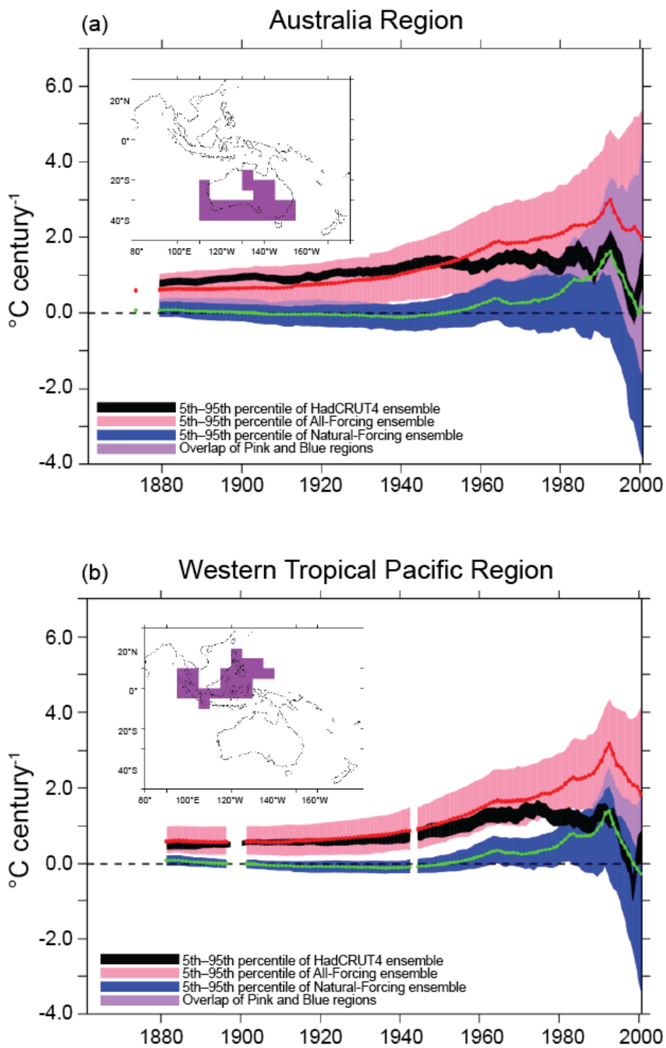

Fig. S8.2. Trends [°C (100 yr^{-1})] in the area-averaged annual-mean surface temperature series in Fig. S8.2 (a,b) as a function of starting year, with all trends ending in 2012. The black curves show trends from observations (HadCRUT4), indicating the 5th–95th percentile range for the HadCRUT4 observed ensemble (Morice et al. 2012). The red curves show the inter-model mean ensemble mean trends from the 10-member subset of the CMIP5 All-Forcing ensemble that provided natural forcing runs. The pink region represents the 'All-Forcing' hypothesis–ie. the 5th–95th percentile range of trends from the All-Forcing runs. The blue-shaded region shows the 5th–95th percentile range of the alternative 'Natural-Forcing-Only' hypothesis using the same 10 models. Purple shading indicates where the pink- and blue-shaded regions overlap. The white spaces in the curves denote years where the initial "start year" was missing due to inadequate spatial or temporal coverage. Temporal coverage was assessed as in Fig. S8.1, and the spatial coverage was assessed for each year by requiring at least 33% non-missing annual means for the region.

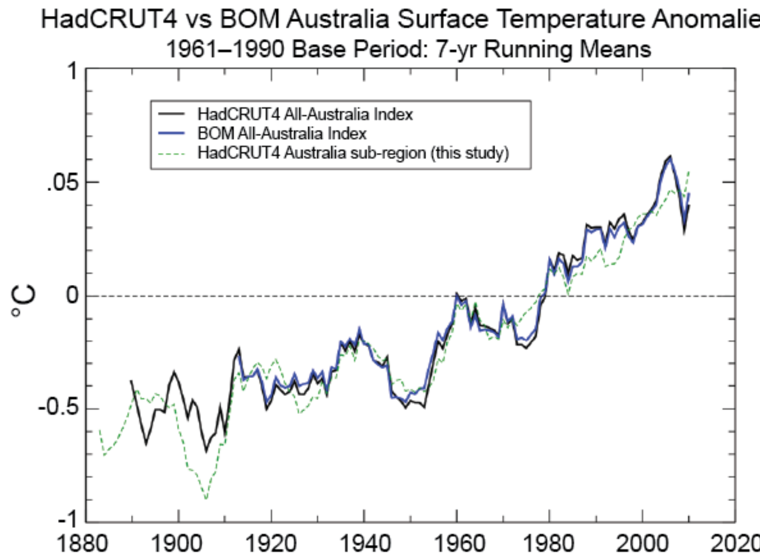

Fig. S8.3. Comparison of all-Australia timeseries of temperature anomalies (relative to 1961–90 base period) for the HadCRUT4 vs. Australian Bureau of Meteorology data set. See text for details. A seven-year running mean was applied to all data sets. The green dashed curve shows the HadCRUT4 data for the sub-region of Australia with near-record high annual-mean temperature anomalies during 2013 (see Figs. 8.1, 8.2 in the main report for region description).

(including Natural Forcing) remains robust to this reference period issue as well.

Considering the far western tropical Pacific region, the use of a later period (1910–49) versus an earlier period (1881–1920) results in a lower observed anomaly magnitude in 2013 by 0.12°C but also, coincidentally, a lower estimated magnitude of the Natural Forcing response in 2012 by almost the same magnitude (0.12°C). Thus, the estimated occurrence rate of the 2013 anomaly in the Natural Forcing distribution would be essentially the same for the 1910–49 base period as for the 1881–1920 base period, due to these offsetting effects, and our conclusions about exceptional nature of the 2013 anomaly compared to Natural Forcing simulations remain robust.

REFERENCES

Adler, R. F., and Coauthors, 2003: The Version 2 Global Precipitation Climatology Project (GPCP) monthly precipitation analysis (1979-Present). *J. Hydrometeor.*, **4**, 1147–1167.

Alexandersson, H., T. Schmith, K. Iden, and H. Tuomenvirta, 1998: Long-term variations of the storm climate over NW Europe. *Global Atmos. Ocean Sys.*, **6**, 97–120.

——, H. Tuomenvirta, T. Schmith, and K. Iden, 2000: Trends of storms in NW Europe derived from an updated pressure data set. *Climate Res.*, **14**, 71–73.

Allan, R., and C. K. Folland, 2012: [Global climate] Atmospheric circulation: Mean sea level pressure [in "State of the Climate 2011"]. *Bull. Amer. Meteor. Soc.*, **93** (7), S35–S36.

——, and B. J. Soden, 2008: Atmospheric warming and the amplification of precipitation extremes. *Science*, **321**, 1484.

Allen, M., 1999: Do-it-yourself climate prediction. *Nature*, **401**, 642.

——, 2003: Liability for climate change. *Nature*, **421**, 891–892.

Andermann, C., L. Longuevergne, S. Bonnet, A. Crave, P. Davy, and R. Gloaguen, 2012: Impact of transient groundwater storage on the discharge of Himalayan rivers. *Nature Geosci.*, **5**, 127–132.

Arblaster, J. M., and L. V. Alexander, 2012: The impact of the El Niño-Southern Oscillation on maximum temperature extremes. *Geophys. Res. Lett.*, **39**, L20702, doi:10.1029/2012GL053409.

Ashfaq, M., Y. Shi, W.-W. Tung, R. J. Trapp, X. Gao, J. S. Pal, and N. S. Diffenbaugh, 2009: Suppression of south Asian summer monsoon precipitation in the 21st century. *Geophys. Res. Lett.*, **36**, L01704, doi:10.1029/2008GL036500.

BAAQMD, 2014: Challenging "Winter Spare the Air" season comes to a close. Bay Area Air Quality Management District, press release, 4 March 2014. [Available online at http://www.baaqmd.gov/~/media/Files/Communications%20and%20Outreach/Publications/News%20Releases/2014/2014-019-WSTA-SEASON-ENDS-030414.ashx?la=en.]

Bacmeister, J. T., M. J. Suarez, and F. R. Robertson, 2006: Rain reevaporation, boundary layer–convection interactions, and Pacific rainfall patterns in an AGCM. *J. Atmos. Sci.*, **63**, 3383–3403.

——, M. F. Wehner, R. B. Neale, A. Gettelman, C. Hannay, P. H. Lauritzen, J. M. Caron, and J. E. Truesdale, 2014: Exploratory high-resolution climate simulations using the Community Atmosphere Model (CAM). *J. Climate*, **27**, 3073–3099.

Balmaseda, M. A., L. Ferranti, F. Molteni, and T. N. Palmer, 2010: Impact of 2007 and 2008 Arctic ice anomalies on the atmospheric circulation: Implications for long-range predictions. *Quart. J. Roy. Meteor. Soc.*, **136**, 1655–1664.

Barnett, T. P., and Coauthors, 2008: Human-induced changes in the hydrology of the western United States. *Science*, **319**, 1080–1083.

Barriopedro, D., E. M. Fischer, J. Lutenbacher, R. M. Trigo, and R. Garcia-Herrera, 2011: The hot summer of 2010: redrawing the temperature record map of Europe. *Science*, **332**, 220–224.

Becker, A., P. Finger, A. Meyer-Christoffer, B. Rudolf, K. Schamm, U. Schneider, and M. Ziese, 2013: A description of the global land-surface precipitation data products of the Global Precipitation Climatology Centre with sample applications including centennial (trend) analysis from 1901 to present. *Earth Syst. Sci. Data*, **5**, 71–99.

Berg, P., J. O. Haerter, P. Thejll, C. Piani, S. Hagemann, and J. H. Christensen, 2009: Seasonal characteristics of the relationship between daily precipitation intensity and surface temperature. *J. Geophys. Res.*, **114**, D18102, doi:10.1029/2009JD012008.

BfG-DWD, 2013: Länderübergreifende Analyse des Juni-Hochwassers 2013. Bundesanstalt für Gewässerkunde, 69 pp. [Available online at http://www.vhw.de/fileadmin/user_upload/Themenfelder/Umweltrecht/2013_09_04_pm_bfg-bericht.pdf.]

Bhend, J., and P. Whetton, 2013: Consistency of simulated and observed regional changes in temperature, sea level pressure and precipitation. *Climatic Change*, **118**, 799–810, doi:10.1007/s10584-012-0691-2.

Bindoff, N. L., and Coauthors, 2014: Detection and attribution of climate change: From global to regional. *Climate Change 2013: The Physical Science Basis*, T. F. Stocker et al., Eds., Cambridge University Press, 867–952.

Blackham, M., 2013: Dust bowled. *Water Atmos.*, **8**, 12–21.

Bladé, I., B. Liebmann, D. Fortuny, and G. J. Oldenborgh, 2012: Observed and simulated impacts of the summer NAO in Europe: Implications for projected drying in the Mediterranean region. *Climate Dyn.*, **39**, 709–727, doi:10.1007/s00382-011-1195-x.

Blunden, J., and D. S. Arndt, Eds., 2014: State of the Climate in 2013. *Bull. Amer. Meteor. Soc.*, **95** (7), S1–S257.

Boé, J., L. Terray, C. Cassou, and J. Najac, 2009: Uncertainties in European summer precipitation changes: Role of large scale circulation. *Climate Dyn.*, **33**, 265–276, doi:10.1007/s00382-008-0474-7.

Borah, N., A. K. Sahai, R. Chattopadhyay, S. Joseph, S. Abhilash, and B. N. Goswami, 2013: A self-organizing map–based ensemble forecast system for extended range prediction of active/break cycles of Indian summer monsoon. *J. Geophys. Res. Atmos.*, **118**, 9022–9034, doi:10.1002/jgrd.50688.

Buisán, S. T., M. A. Sanz, and J. I. López-Moreno, 2014: Spatial and temporal variability of winter snow and precipitation days in the western and central Spanish Pyrenees. *Int. J. Climatol.*, in press, doi:10.1002/joc.3978.

Bureau of Meteorology, 2012: State of the Climate 2012. [Available online at http://www.csiro.au/Outcomes/Climate/Understanding/State-of-the-Climate-2012.aspx.]

——, 2013a: Extreme heat in January 2013. Bureau of Meteorology Special Climate Statement 43, 19 pp. [Available online at http://www.bom.gov.au/climate/current/statements/scs43e.pdf.]

——, 2013b: Australia's warmest September on record. Bureau of Meteorology Special Climate Statement 46, 26 pp. [Available online at http://www.bom.gov.au/climate/current/statements/scs46.pdf.]

——, 2014: Annual Climate Report 2013. Bureau of Meteorology (Australia), 31 pp. [Available online at http://www.bom.gov.au/climate/annual_sum/2013/index.shtml.]

CAL FIRE, 2014: Drought prompts CAL FIRE to increase statewide staffing: Expected prolonged, elevated threat of wildfire due to dry conditions. CAL FIRE, news release, 28 January 2014. [Available online at http://www.fire.ca.gov/communications/downloads/newsreleases/2014/2014_Drought_Staffing.pdf.]

Carrera, M., R. Higgins, and V. Kousky, 2004: Downstream weather impacts associated with atmospheric blocking over the northeast Pacific. *J. Climate*, **17**, 4823–4840.

Cassou, C., 2008: Intraseasonal interaction between the Madden–Julian Oscillation and the North Atlantic Oscillation. *Nature*, **455**, 523–527.

Cattiaux, J., and P. Yiou, 2012: Contribution of atmospheric circulation to remarkable European temperatures of 2011. *Bull. Amer. Meteor. Soc.*, **93**, 1054–1057.

——, R. Vautard, C. Cassou, P. Yiou, V. Masson-Delmotte, and F. Codron, 2010: Winter 2010 in Europe: A cold extreme in a warming climate. *Geophys. Res. Lett.*, **37**, L20704, doi:10.1029/2010gl044613.

Cayan, D., and J. Roads, 1984: Local relationships between United States West Coast precipitation and monthly mean circulation parameters. *Mon. Wea. Rev.*, **112**, 1276–1282.

CDFW, 2014: CDFW puts closures in effect on some rivers, recommends further changes to the Fish and Game Commission. *California Department of Fish and Wildlife News*, 29 January 2014. [Available online at http://cdfgnews.wordpress.com/2014/01/29/cdfw-puts-closures-in-effect-on-some-rivers-recommends-further-changes-to-the-fish-and-game-commission.]

Chattopadhyay, R., A. K. Sahai, and B. N. Goswami, 2008: Objective identification of nonlinear convectively coupled phases of monsoon intraseasonal oscillation: Implications for prediction. *J. Atmos. Sci.*, **65**, 1549–1569.

Chen, S., and D. Cayan, 1994: Low-frequency aspects of the large-scale circulation and West Coast United States temperature/precipitation fluctuations in a simplifed general circulation model. *J. Climate*, **7**, 1668–1683.

Christidis, N., and P. A. Stott, 2014: Change in the odds of warm years and seasons due to anthropogenic influence on the climate. *J. Climate*, **27**, 2607–2621.

——, ——, and S. J. Brown, 2011: The role of human activity in the recent warming of extremely warm daytime temperatures. *J. Climate*, **24**, 1922–1930.

——, ——, G. S. Jones, H. Shiogama, T. Nozawa, and J. Luterbacher, 2012: Human activity and warm seasons in Europe. *Int. J. Climatol.*, **32**, 225–239.

——, ——, A. A. Scaife, A. Arribas, G. S. Jones, D. Copsey, J. R. Knight, and W. J. Tennant, 2013: A new HadGEM3-A-based system for attribution of weather- and climate-related extreme events. *J. Climate*, **26**, 2756–2783.

CIB, cited 2013: Central European flooding 2013. EURO4M Climate Indicator Bulletin. [Available online at http://cib.knmi.nl/mediawiki/index.php/Central_European_flooding_2013.]

Clark, A., B. Mullan, and A. Porteous, 2011: Scenarios of regional drought under climate change. National Institute of Water & Atmospheric Research, 135 pp. [Available online at http://www.niwa.co.nz/sites/niwa.co.nz/files/slmacc_drought_sldr093_june2011.pdf.]

CMA, 2014: *China Climate Bulletin for 2013.* China Meteorological Administration, 50 pp.

Compo, G. P., and P. D. Sardeshmukh, 2010: Removing ENSO-related variations from the climate record. *J. Climate*, **23**, 1597–1978.

Coumou, D., and S. Rahmstorf, 2012: A decade of weather extremes. *Nature Climate Change*, **2**, 491–496, doi:10.1038/NCLIMATE1452.

Dai, A., 2008: Temperature and pressure dependence of the rain-snow phase transition over land and ocean. *Geophys. Res. Lett.*, **35**, L12802, doi:10.1029/2008GL033295.

——, 2011: Drought under global warming: a review. *Wiley Interdiscip. Rev.: Climate Change*, **2**, 45–65.

——, 2013: The influence of the Inter-decadal Pacific Oscillation on US precipitation during 1923-2010. *Climate Dyn.*, **41**, 633–646.

Daithi, S., 2013: Boundary conditions for the C20C Detection and Attribution project: The ALL-Hist/est1 and NAT-Hist/CMIP5-est1 scenarios. International CLIVAR C20C+ Detection and Attribution Project, 18 pp. [Available online at http://portal.nersc.gov/c20c/input_data/C20C-DandA_dSSTs_All-Hist-est1_Nat-Hist-CMIP5-est1.pdf.]

Dangendorf, S., S. Müller-Navarra, J. Jensen, F. Schenk, T. Wahl, and R. Weisse, 2014: North Sea storminess from a novel storm surge record since AD 1843. *J. Climate*, **27**, 3582–3595.

Dee, D. P., and Coauthors, 2011: The ERA-Interim reanalysis: Configuration and performance of the data assimilation system. *Quart. J. Roy. Meteor. Soc.*, **137**, 553–597, doi:10.1002/qj.828.

DEFRA, 2013: Defra to meet the cost of removing sheep killed in snow, Department for Environment, Food & Rural Affairs, press release, 15 May 2013. [Available online at https://www.gov.uk/government/news/defra-to-meet-the-cost-of-removing-sheep-killed-in-snow.]

Deser, C., A. S. Phillips, and M. A. Alexander, 2010: Twentieth century tropical sea surface temperature trends revisited. *Geophys. Res. Lett.*, **37**, L10701, doi:10.1029/2010GL043321.

Deutschländer, T., K. Friedrich, S. Haeseler, and C. Lefebvre, 2013: Severe storm XAVER across northern Europe from 5 to 7 December 2013. Deutscher Wetterdienst, 19 pp. [Available online at http://www.dwd.de/bvbw/generator/DWDWWW/Content/Oeffentlichkeit/KU/KU2/KU24/besondere__ereignisse__global/stuerme/englischeberichte/201312__XAVER__europe,templateId=raw,property=publicationFile.pdf/201312_XAVER_europe.pdf.]

Dobhal, D. P., A. K. Gupta, M. Mehta, and D. D. Khandelwal, 2013: Kedarnath disaster: Facts and plausible causes. *Current Sci.*, **105**, 171–174.

Dole, R., J. Perlwitz, J. Eischeid, P. Pegion, T. Zhang, X. W. Quan, T. Xu, and D. Murray, 2011: Was there a basis for anticipating the 2010 Russian heat wave? *Geophys. Res. Lett.*, **38**, L06702, doi:10.1029/2010GL046582.

Donat, M. G., and Coauthors, 2013: Updated analyses of temperature and precipitation extreme indices since the beginning of the twentieth century: The HadEX2 dataset. *J. Geophys. Res. Atmos.*, **118**, 2098–2118, doi:10.1002/jgrd.50150.

Dong, B.-W., R. T. Sutton, and T. Woollings, 2013a: The extreme European summer 2012 (in "Explaining Extreme Events of 2012 from a Climate Perspective"). *Bull. Amer. Meteor. Soc.*, **94** (9), S28–S32.

——, ——, ——, and K. Hodges, 2013b: Variability of the North Atlantic summer stormtrack: Mechanisms and impacts. *Environ. Res. Lett.*, **8**, 034037, doi:10.1088/1748-9326/8/3/034037.

Douville, H., S. Bielli, C. Cassou, M. Dequé, N. M. J. Hall, S. Tyteca, and A. Voldoire, 2011: Tropical influence on boreal summer mid-latitude stationary waves. *Climate Dyn.*, **38**, 1783–1798.

Dube, A., R. Ashrit, A. Ashish, K. Sharma, G. R. Iyengar, E. N. Rajagopal, and S. Basu, 2013: Performance of NCMRWF forecast models in predicting the Uttarakhand heavy rainfall event during 17–18 June 2013. [India] National Centre for Medium Range Weather Forecasting Research Report NMRF/RR/08/2013, 35 pp. [Available online at http://www.ncmrwf.gov.in/ncmrwf/KEDARNATH_REPORT_FINAL.pdf.]

——, ——, ——, ——, ——, ——, and ——, 2014: Forecasting the heavy rainfall during Himalayan flooding - June 2013. *Wea. Climate Extremes*, **4**, 22–34, doi:10.1016/j.wace.2014.03.004.

Dubey, C. S., D. P. Shukla, A. S. Ningreichon, and A. L. Usham, 2013: Orographic control of the Kedarnath disaster. *Current Sci.*, **105**, 1474–1476.

Durga Rao, K. H. V., V. Venkateshwar Rao, V. K. Dadhwal, and P. G. Diwakar, 2014: Kedarnath flash floods: A hydrological and hydraulic simulation study. *Current Sci.*, **106**, 598–603.

DWR, 2013: DWR experimental winter outlook for water year 2014: Sees mostly dry conditions for California. California Department of Water Resources, news release, 27 November 2013. [Available online at http://www.water.ca.gov/news/newsreleases/2013/112513.pdf.]

——, 2014: DWR drops state water project allocation to zero, seeks to preserve remaining supplies. California Department of Water Resources, news release, 31 January 2014. [Available online at http://www.water.ca.gov/news/newsreleases/2014/013114pressrelease.pdf.]

El Kenawy, A., J. I. López-Moreno, and S. M. Vicente-Serrano, 2012: Trend and variability of surface air temperature in northeastern Spain (1920-2006): Linkage to atmospheric circulation. *Atmos. Res.*, **106**, 159–180.

Favre, A., and A. Gershunov, 2009: North Pacific cyclonic and anticyclonic transients in a global warming context: Possible consequences for Western North American daily precipitation and temperature extremes. *Climate Dyn.*, **32**, 969–987.

Feser, F., R. Weisse, and H. von Storch, 2001: Multi-decadal atmospheric modeling for Europe yields multi-purpose data. *Eos, Trans. Amer. Geophys. Union*, **82**, 305–310.

——, M. Barcikowska, O. Krueger, F. Schenk, R. Weisse, and L. Xia, 2014: Storminess over the North Atlantic and northwestern Europe - A review. *Quart. J. Roy. Meteor. Soc.*, in press, doi:10.1002/qj.2364.

Field, C. B., and Coauthors, Eds., 2012: *Managing the Risks of Extreme Events and Disasters to Advance Climate Change Adaptation*. Cambridge University Press, 582 pp.

Fischer, E. M., U. Beyerle, and R. Knutti, 2013: Spatial aggregation reveals robust projections in climate extremes. *Nature Climate Change*, **3,** 1033–1038, doi:10.1038/NCLIMATE2051.

Folland, C. K., J. Knight, H. W. Linderholm, D. Fereday, S. Ineson, and J. W. Hurrell, 2009: The summer North Atlantic oscillation: Past, present, and future. *J. Climate*, **22**, 1082–1103.

Francis, J. A., and S. J. Vavrus, 2012: Evidence linking Arctic amplification to extreme weather in mid-latitudes. *Geophys. Res. Lett.*, **39**, L06801, doi:10.1029/2012GL051000.

Franke, R., 2009: Die nordatlantischen Orkantiefs seit 1956. *Naturwiss. Rundsch.*, **62**, 349–356, updated.

Fyfe, J. C., N. P. Gillett, and G. J. Marshall, 2012: Human influence on extratropical southern hemisphere summer precipitation. *Geophys. Res. Lett.*, **39**, L23711, doi:10.1029/2012GL054199.

——, ——, and F. W. Zwiers, 2013: Overestimated global warming over the past 20 years. *Nature Climate Change*, **3**, 767–769.

Gershunov, A., and D. Cayan, 2003: Heavy daily precipitation frequency over the contiguous United States: Sources of climatic variability and seasonal predictability. *J. Climate*, **16**, 2752–2765.

Geyer, B., 2014: High-resolution atmospheric reconstruction for Europe 1948–2012: coastDat2. *Earth Sys. Sci. Data*, **6**, 147–164, doi:10.5194/essd-6-147-2014.

Ghosh, S., D. Das, S.-C. Kao, and A. R. Ganguly, 2012: Lack of uniform trends but increasing spatial variability in observed Indian rainfall extremes. *Nature Climate Change*, **2**, 86–91.

Goswami, B. N., V. Venugopal, D. Sengupta, M. S. Madhusoodanan, and P. K. Xavier, 2006: Increasing trend of extreme rain events over India in a warming environment. *Science*, **314**, 1442–1445.

Graham, R. A., and R. H. Grumm, 2010: Utilizing normalized anomalies to assess synoptic-scale weather events in the western United States. *Wea. Forecasting*, **25**, 428–445.

Grams, C. M., H. Binder, S. Pfahl, N. Piaget, and H. Wernli, 2014: Atmospheric processes triggering the central European floods in June 2013. *Nat. Hazards Earth Syst. Sci.*, **14**, 1691–1702, doi:10.5194/nhess-14-1691-2014.

Graves, C. E., J. T. Moore, M. J. Singer, and S. Ng, 2003: Band on the run - Chasing the physical processes associated with heavy snowfall. *Bull. Amer. Meteor. Soc.*, **84**, 990–994.

Grumm, R. H., and R. Hart, 2001: Standardized anomalies applied to significant cold season weather events: Preliminary findings. *Wea. Forecasting*, **16**, 736–754.

Haeseler, S., and Coauthors, 2013: Heavy storm CHRISTIAN on 28 October 2013. Deutscher Wetterdienst, 20 pp. [Available online at http://www.dwd.de/bvbw/generator/DWDWWW/Content/Oeffentlichkeit/KU/KU2/KU24/besondere__ereignisse__global/stuerme/englischeberichte/20131028__CHRISTIAN__europe,templateId=raw,property=publicationFile.pdf/20131028_CHRISTIAN_europe.pdf.]

Hamill, T., 2014: Performance of operational model precipitation forecast guidance during the 2013 Colorado Front-Range floods. *Mon. Wea. Rev.*, **142**, 2609–2618.

Hansen, W. R., B. J. Chronic, and J. Matelock, 1978: Climatography of the Front Range urban corridor and vicinity, Colorado. USGS Professional Paper 1019, 59 pp. [Available online at http://pubs.usgs.gov/pp/1019/report.pdf.]

Hart, R. E., and R. H. Grumm, 2001: Using normalized climatological anomalies to rank synoptic-scale events objectively. *Mon. Wea. Rev.*, **129**, 2426–2442.

Hartmann, D. L., and Coauthors, 2014: Observations: Atmosphere and surface. *Climate Change 2013: The Physical Science Basis,* T. F. Stocker et al., Eds., Cambridge University Press, 159–254.

Hasselmann, K., 1979: On the signal-to-noise problem in atmospheric response studies. *Meteorology over the Tropical Oceans*, B. D. Shaw, Ed., Royal Meteorological Society, 251–259.

Haylock, M. R., N. Hofstra, A. M. G. Klein Tank, E. J. Klok, P. D. Jones, and M. New, 2008: A European daily high-resolution gridded dataset of surface temperature and precipitation for 1950–2006. *J. Geophys. Res.*, **113**, D20119, doi:10.1029/2008JD010201.

Hegerl, G., and F. Zwiers, 2011: Use of models in detection and attribution of climate change. *Wiley Interdiscip. Rev.: Climate Change*, **2**, 570–591.

——, O. Hoegh-Guldberg, G. Casassa, M. P. Hoerling, R. S. Kovats, C. Parmesan, D. W. Pierce, and P. A. Stott, 2009: Good practice guidance paper on detection and attribution related to anthropogenic climate change. IPCC Expert Meeting on Detection and Attribution Related to Anthropogenic Climate Change, T. F. Stocker et al., Eds., University of Bern, Switzerland, 1–8. [Available online at https://www.ipcc-wg1.unibe.ch/guidancepaper/IPCC_D&A_GoodPracticeGuidancePaper.pdf.]

Hendon, H. H., D. W. J. Thompson, and M. C. Wheeler, 2007: Australian rainfall and surface temperature variations associated with the Southern Hemisphere annular mode. *J. Climate*, **20**, 2452–2467.

——, E.-P. Lim, J. M. Arblaster, and D. T. L. Anderson 2014: Causes and predictability of the record wet spring over Australia in 2010. *Climate Dyn.,* **42**, 1155–1174.

Hewitson, B. C., and R. G. Crane, 2002: Self-organizing maps: Applications to synoptic climatology. *Climate Res.*, **22**, 13–26.

Hewitt, H. T., D. Copsey, I. D. Culverwell, C. M. Harris, R. S. R. Hill, A. B. Keen, A. J. McLaren, and E. C. Hunke, 2011: Design and implementation of the infrastructure of HadGEM3: The next-generation Met Office climate modelling system. *Geosci. Model Dev.*, **4**, 223–253.

Hirabayashi, Y., R. Mahendran, S. Koirala, L. Konoshima, D. Yamazaki, S. Watanabe, H. Kim, and S. Kanaes, 2013: Global flood risk under climate change. *Nature Climate Change*, **3**, 816–821.

Hirsch, R. M., and K. R. Ryberg, 2012: Has the magnitude of floods across the USA changed with global CO2 levels? *Hydrolog. Sci. J.*, **57**, 1–9, doi:10.1080/02626667.2011.621895.

Hoerling, M., J. Eischeid, J. Perlwitz, X. Quan, T. Zhang, and P. Pegion, 2012: On the increased frequency of Mediterranean drought. *J. Climate*, **25**, 2146–2161.

——, and Coauthors, 2013: Anatomy of an extreme event. *J. Climate*, **26**, 2811–2832.

Hong, C.-C., H.-H. Hsu, N.-H. Lin, and H. Chiu, 2011: Roles of European blocking and tropical-extratropical interaction in the 2010 Pakistan flooding. *Geophys. Res. Lett.*, **38**, L13806, doi:10.1029/2011GL047583.

Hoskins, B. J., and K. I. Hodges, 2002: New perspectives on the Northern Hemisphere winter storm tracks. *J. Atmos. Sci.*, **59**, 1041–1061.

Houze, R. A., K. L. Rasmussen, S. Medina, S. R. Brodzik, and U. Romatschke, 2011: Anomalous atmospheric events Leading to the summer 2010 floods in Pakistan. *Bull. Amer. Meteor. Soc.*, **92**, 291–298.

HPRC, cited 2014: High Plains Regional Center - Current climate summary maps. [Available online at http://www.hprcc.unl.edu/.]

Hudson, D., A. G. Marshall, Y. Yin, O. Alves, and H. H. Hendon, 2013: Improving intraseasonal prediction with a new ensemble generation strategy. *Mon. Wea. Rev.*, **141**, 4429–4449.

Huffington Post, 2014: The costs of California's bellwether drought: What can we expect? [Available online at http://www.huffingtonpost.com/peter-h-gleick/the-costs-of-californias_b_4747043.html.]

Hurrell, J. W., and C. Deser, 2009: North Atlantic climate variability: The role of the North Atlantic Oscillation. *J. Marine Sys.*, **79**, 231–244.

——, and Coauthors, 2013: The Community Earth System Model: A framework for collaborative research. *Bull. Amer. Meteor. Soc.*, **94**, 1339–1360.

Johnson, N. C., 2013: How many ENSO flavors can we distinguish? *J. Climate*, **26**, 4816–4827.

Jones, D. A., W. Wang, and R. Fawcett, 2009: High-quality spatial climate data-sets for Australia. *Aust. Meteor. Oceanogr. J.*, **58**, 233–248.

Jones, P. D., D. H. Lister, T. J. Osborn, C. Harpham, M. Salmon, and C. P. Morice, 2012: Hemispheric and large-scale land surface air temperature variations: An extensive revision and an update to 2010. *J. Geophys. Res.*, **117**, D05127, doi:10.1029/2011JD017139.

Joseph, S., and Coauthors, 2014: North Indian heavy rainfall event during June 2013: Diagnostics and extended range prediction. *Climate Dyn.*, in press, doi:10.1007/s00382-014-2291-5.

Junker, N. W., R. H. Grumm, R. Hart, L. F. Bosart, K. M. Bell, and F. J. Pereira, 2008: Use of normalized anomaly fields to anticipate extreme rainfall in the mountains of northern California. *Wea. Forecasting*, **23**, 336–356.

Jurewicz, M. L., and M. S. Evans, 2004: A comparison of two banded, heavy snowstorms with very different synoptic settings. *Wea. Forecasting*, **19**, 1011–1028.

Kalnay, E., and Coauthors, 1996: The NCEP/NCAR 40-Year Reanalysis Project. *Bull. Amer. Meteor. Soc.*, **77**, 437–471.

Karoly, D. J., 2009: The recent bushfires and extreme heat wave in southeast Australia. *Bull. Aust. Meteor. Oceanogr. Soc.*, **22**, 10–13.

——, and K. Braganza, 2005: A new approach to detection of anthropogenic temperature changes in the Australian region. *Meteor. Atmos. Phys.,* **89**, 57–67.

——, and Coauthors, 2012: Science underpinning the prediction and attribution of extreme events. WCRP Grand Challenge white paper, 5 pp. [Available online at http://www.wcrp-climate.org/documents/GC_Extremes.pdf.]

Kerr, R., 2013: In the hot seat. *Science*, **342**, 688–689.

Kim, Y. H., M.-K. Kim, and W.-S. Lee, 2008: An investigation of large-scale climate indices with the influence of temperature and precipitation variation in Korea. *Atmosphere*, **18**, 83–95. (In Korean with English abstract.)

Kistler, R., and Coauthors, 2001: The NCEP-NCAR 50-year reanalysis: Monthly means CD-ROM and documentation. *Bull. Amer. Meteor. Soc.*, **82**, 247–267.

Klein-Tank, A. M. G., and Coauthors, 2002: Daily dataset of 20th-century surface air temperature and precipitation series for the European Climate Assessment. *Int. J. Climatol.*, **22**, 1441–1453.

Knutson, T. R., F. Zeng, and A. T. Wittenberg, 2013a: Multimodel assessment of regional surface temperature trends: CMIP3 and CMIP5 Twentieth Century simulations. *J. Climate*, **26**, 8709–8743.

——, ——, and ——, 2013b: The extreme March 2012 warm anomaly over the eastern United States: Global context and multimodel trend analysis [in "Explaining Extreme Events of 2012 from a Climate Perspective"]. *Bull. Amer. Meteor. Soc.*, **94** (9), S13–S17.

Knutti, R., and J. Sedláček, 2013: Robustness and uncertainties in the new CMIP5 climate model projections. *Nature Climate Change*, **3**, 369–373.

Kohonen, T., 2001: *Self-Organizing Maps.* 3rd ed. Springer Series in Information Sciences, Vol. 30, Springer, 501 pp.

Krishnamurthy, C. K. B., U. Lall, and H.-H. Kwon, 2009: Changing frequency and intensity of rainfall extremes over India from 1951 to 2003. *J. Climate*, **22**, 4737–4746.

Kumar, A., H. Wang, W. Wang, Y. Xue, and Z.-Z. Hu, 2013: Does knowing the oceanic PDO phase help predict the atmospheric anomalies in subsequent months? *J. Climate*, **26**, 1268–1285.

Kunkel, K. E., and Coauthors, 2013: Monitoring and understanding trends in extreme storms: State of knowledge. *Bull. Amer. Meteor. Soc.*, **94**, 499–514.

Lamarque, J.-F., and Coauthors, 2010: Historical (1850–2000) gridded anthropogenic and biomass burning emissions of reactive gases and aerosols: Methodology and application. *Atmos. Chem. Phys.*, **10**, 7017–7039, doi:10.5194/acp-10-7017-2010.

Langford, S., S. Stevenson, and D. Noone, 2014: Analysis of low-frequency precipitation variability in CMIP5 historical simulations for southwestern North America. *J. Climate*, **27**, 2735–2756.

Lau, W. K. M., and K.-M. Kim, 2011: The 2010 Pakistan flood and Russian heat wave: Teleconnection of hydrometeorological extremes. *J. Hydrometeor.*, **13**, 392–403.

Lewis, S. C., and D. J. Karoly, 2013: Anthropogenic contributions to Australia's record summer temperatures of 2013. *Geophys. Res. Lett.*, **40**, 3705–3709, doi:10.1002/grl.50673.

Li, C., and M. Yanai, 1996: The onset and interannual variability of the Asian summer monsoon in relation to land–sea thermal contrast. *J. Climate*, **9**, 358–375.

Li, H., J. Sheffield, and E. F. Wood, 2010a: Bias correction of monthly precipitation and temperature fields from Intergovernmental Panel on Climate Change AR4 models using equidistant quantile matching. *J. Geophys. Res.*, **115**, D10101, doi:10.1029/2009JD012882.

——, A. Dai, T. Zhou, and J. Lu, 2010b: Responses of East Asian summer monsoon to historical SST and atmospheric forcing during 1950–2000. *Climate Dyn.*, **34**, 501–514.

Lindenberg, J., H.-T. Mengelkamp, and G. Rosenhagen, 2012: Representativity of near surface wind measurements from coastal stations at the German Bight. *Meteor. Z.*, **21**, 99–106.

López-Moreno, J. I., 2005: Recent variations of snowpack depth in the Central Spanish Pyrenees. *Arct. Antarct. Alp. Res.*, **37**, 253–260.

——, and S. M. Serrano-Vicente, 2007: Atmospheric circulation influence on the interannual variability of snowpack in the Spanish Pyrenees during the second half of the twentieth century. *Nordic Hydrol.*, **38**, 38–44.

——, ——, and S. Lanjeri, 2007: Mapping of snowpack distribution over large areas using GIS and interpolation techniques. *Climate Res.*, **33**, 257–270.

——, ——, S. Beguería, A. M. El Kenawy, and M. Angulo, 2010: Trends in daily precipitation on the north-eastern Iberian Peninsula, 1955-2006. *Int. J. Climatol.*, **120**, 248–257.

Lorenz, R., E. B. Jaeger, and S. I. Seneviratne, 2010: Persistence of heat waves and its link to soil moisture memory. *Geophys. Res. Lett.,* **37**, L09703, doi:10.1029/2010GL042764.

Lott, F. C., N. Christidis, and P. A. Stott, 2013: Can the 2011 East African drought be attributed to human-induced climate change? *Geophys. Res. Lett.*, **40**, 1177–1181.

Mantua, N. J., S. R. Hare, Y. Zhang, J. M. Wallace, and R. C. Francis, 1997: A Pacific interdecadal climate oscillation with impacts on salmon production. *Bull. Amer. Meteor. Soc.*, **78**, 1069–1079.

Marshall, A. G., D. Hudson, M. C. Wheeler, O. Alves, H. H. Hendon, M. J. Pook, and J. S. Risbey, 2013: Intra-seasonal drivers of extreme heat over Australia in observations and POAMA-2. *Climate Dyn.*, doi:10.1007/s00382-013-2016-1.

Martin, J. E., 1999: Quasigeostrophic forcing of ascent in the occluded sector of cyclones and the trowal airstream. *Mon. Wea. Rev.*, **127**, 70–88.

Marty, C., 2008: Regime shift of snow days in Switzerland. *Geophys. Res. Lett.*, **35**, L12501, doi:10.1029/2008GL033998.

Marvel, K., and C. Bonfils, 2013: Identifying external influences on global precipitation. *Proc. Natl. Acad. Sci. USA*, **110**, 19301–19306.

Massey, N., and Coauthors, 2014: weather@home – development and validation of a very large ensemble modelling system for probabilistic event attribution. *Quart. J. Roy. Meteor. Soc.*, in press, doi:10.1002/qj.2455.

Mastrandrea, M. D., K. J. Mach, G.-K. Plattner, O. Edenhofer, T. F. Stocker, C. B. Field, K. L. Ebi, and P. R. Matschoss, 2011: The IPCC AR5 guidance note on consistent treatment of uncertainties: a common approach across the working groups. *Climate Change*, **108**, 675–691.

Matulla, C., W. Schöner, H. Alexandersson, H. von Storch, and X. Wang, 2007: European storminess: Late nineteenth century to present. *Climate Dyn.*, **31**, 125–130.

Mayes, B. E., J. M. Boustead, M. O'Malley, S. M. Fortin, and R. H. Grumm, 2009: Utilizing standardized anomalies to assess synoptic scale weather events in the central United States. Preprints, *23rd Conf. on Weather Analysis and Forecasting*, Omaha, NE, Amer. Meteor. Soc., 16B.3. [Available online at http://ams.confex.com/ams/pdfpapers/154217.pdf.]

McCabe, G. J., and M. D. Dettinger, 1999: Decadal variations in the strength of ENSO teleconnections with precipitation in the western United States. *Int. J. Climatol.*, **19**, 1399–1410.

McKee, T. B., and N. J. Doesken, 1997: Colorado Extreme Storm Precipitation Data Study. Climatology Rep. 97-1, Colorado Climate Center, Colorado State University, 109 pp. [Available online at http://climate.colostate.edu/pdfs/Climo_97-1_Extreme_ppt.pdf.]

Menne, M., I. Durre, R. Vose, B. Gleason, and T. Houston, 2012: An overview of the Global Historical Climatology Network-Daily database. *J. Atmos. Oceanic Technol.*, **29**, 897–910.

Met Office, cited 2014: Hot dry spell July 2013. [Available online at http://www.metoffice.gov.uk/climate/uk/interesting/2013-heatwave.]

Michelangeli, P.-A., R. Vautard, and B. Legras, 1995: Weather regimes: Recurrence and quasi-stationarity. *J. Atmos. Sci.*, **52**, 1237–1256.

Min, S.-K., X. Zhang, F. W. Zwiers, and G. C. Hegerl, 2011: Human contribution to more-intense precipitation extremes. *Nature*, **470**, 378–381, doi:10.1038/nature09763.

——, ——, ——, H. Shiogama, Y.-S. Tung, and M. Wehner, 2013: Multi-model detection and attribution of extreme temperature changes. *J. Climate*, **26**, 7430–7451.

Mishra, A., and J. Srinivasan, 2013: Did a cloud burst occur in Kedarnath during 16 and 17 June 2013. *Current Sci.*, **105**, 1351–1352.

Mitchell, T., and W. Blier, 1997: The variability of wintertime precipitation in the region of California. *J. Climate*, **10,** 2261–2276.

Molod, A., L. Takacs, M. Suarez, J. Bacmeister, I.-S. Song, and A. Eichmann, 2012: The GEOS-5 Atmospheric General Circulation Model: Mean climate and development from MERRA to Fortuna**.** NASA Tech. Rep. Series on Global Modeling and Data Assimilation, NASA TM—2012-104606, Vol. 28, 117 pp.

Moore, J. T., C. E. Graves, S. Ng, and J. L. Smith, 2005: A process-oriented methodology toward understanding the organization of an extensive mesoscale snowband: A diagnostic case study of 4–5 December 1999. *Wea. Forecasting*, **20**, 35–50.

Morak, S., G. C. Hegerl, and J. Kenyon, 2011: Detectable regional changes in the number of warm nights. *Geophys. Res. Lett.*, **38**, L17703, doi:10.1029/2011GL048531.

——, ——, and N. Christidis, 2013: Detectable changes in the frequency of temperature extremes. *J. Climate*, **26**, 1561–1574.

Morice, C. P., J. J. Kennedy, N. A. Rayner, and P. D. Jones, 2012: Quantifying uncertainties in global and regional temperature change using an ensemble of observational estimates: The HadCRUT4 dataset. *J. Geophys. Res.*, **117**, D08101, doi:10.1029/2011JD017187.

Mudelsee, M., M. Börngen, G. Tetzlaff, and U. Grünewald, 2003: No upward trends in the occurrence of extreme floods in central Europe. *Nature*, **425**, 166–169.

Nairn, J., and R. Fawcett, 2013: Defining heatwaves: Heatwave defined as a heat impact event servicing all community and business sectors in Australia. CAWCR Technical Report No. 060, 84 pp. [Available online at http://www.cawcr.gov.au/publications/technicalreports/CTR_060.pdf.]

Namias, J., 1978a: Recent drought in California and western Europe. *Rev. Geophys.*, **16**, 435–458.

——, 1978b: Multiple causes of the North American abnormal winter 1976–1977. *Mon. Wea. Rev.*, **106**, 279–295.

NASA Earth Observatory, cited 2014: MODIS TERRA imagery. [Available online at http://earthobservatory.nasa.gov/IOTD/view.php?id=82910.]

NCDC, 2005: *Storm Data*. NOAA/NESDIS National Climatic Data Center, **47** (10), 132 pp. [Available online at http://www.ncdc.noaa.gov/IPS/sd/sd.html.]

NCLIMDIV, 2014: NOAA's gridded climate divisional dataset. National Climatic Data Center, Asheville, NC, digital media, retrieved 05 June 2014. [Available online at http://www.ncdc.noaa.gov/cag.]

Neelin, J. D., B. Langenbrunner, J. E. Meyerson, A. Hall, and N. Berg, 2013: California winter precipitation change under global warming in the Coupled Model Intercomparison Project Phase 5 ensemble. *J. Climate*, **26**, 6238–6256.

New Zealand Treasury, 2013: Budget economic and fiscal update 2013. New Zealand Treasury, 176 pp. [Available online at http://www.treasury.govt.nz/budget/forecasts/befu2013/befu13-whole.pdf.]

Nicholls, N., 2004: The changing nature of Australian droughts. *Climatic Change*, **63**, 323–336.

NIDIS, cited 2014: National Integrated Drought Information System drought portal. [Available online at http://www.drought.gov/drought/news/ca-governor-signs-687-million-drought-plan.]

Nitschke, M., G. R. Tucker, and P. Bi, 2007: Morbidity and mortality during heatwaves in metropolitan Adelaide. *Med. J. Aust.*, **187**, 662–665.

NOAA, 2013: State of the climate: Global analysis for May 2013. [Available online at http://www.ncdc.noaa.gov/sotc/global/2013/5.]

NOAA NCDC, 2014: National overview: February 2014. [Available online at https://www.ncdc.noaa.gov/sotc/national/2014/2.]

Novak, D. R., L. F. Bosart, D. Keyser, and J. S. Waldstreicher, 2004: An observational study of cold season–banded precipitation in northeast U.S. cyclones. *Wea. Forecasting*, **19**, 993–1010.

Ogawa, F., H. Nakamura, K. Nishii, T. Miyasaka, and A. Kuwano-Yoshida, 2012: Dependence of the climatological axial latitudes of the tropospheric westerlies and storm tracks on the latitude of an extratropical oceanic front. *Geophys. Res. Lett.*, **39**, L05804, doi:10.1029/2011GL049922.

O'Gorman, P. A., and T. Schneider, 2009: The physical basis for increases in precipitation extremes in simulations of 21st-century climate change. *Proc. Natl. Acad. Sci. USA*, **106**, 14773–14777.

Omrani, N.-E., N. S. Keenlyside, J. Bader, and E. Manzini, 2014: Stratosphere key for wintertime atmospheric response to warm Atlantic decadal conditions. *Climate Dyn.*, **42**, 649–663.

Onogi, K., and Coauthors, 2007: The JRA-25 reanalysis. *J. Meteor. Soc. Japan*, **85**, 369–432.

Otto, F. E. L., N. Massey, G. J. van Oldenborgh, R. G. Jones, and M. R. Allen, 2012: Reconciling two approaches to attribution of the 2010 Russian heat wave. *Geophys. Res. Lett.*, **39**, L04702, doi:10.1029/2011GL050422.

Pall, P., T. Aina, D. A. Stone, P. A. Stott, T. Nozawa, A. G. J. Hilberts, D. Lohmann, and M. R. Allen, 2011: Anthropogenic greenhouse gas contribution to flood risk in England and Wales in autumn 2000. *Nature*, **470**, 382–385, doi:10.1038/nature09762.

Pekárová, P., D. Halmová, V. B. Mitková, P. Miklánek, J. Pekár, and P. Škoda, 2013: Historic flood marks and flood frequency analysis of the Danube River at Bratislava, Slovakia. *J. Hydrol. Hydromech.*, **61**, 326–333.

Perkins, S. E., and L. V. Alexander, 2013: On the measurement of heat waves. *J. Climate*, **26**, 4500–4517.

——, and E. M. Fischer, 2013: The usefulness of different realizations from the model evaluation of regional trends in heat waves. *Geophys. Res. Lett.,* **40**, 5793–5797, doi:10.1002/2013GL057833.

Peters, G. P., and Coauthors, 2012: The challenge to keep global warming below 2°C. *Nature Climate Change*, **3**, 4–6, doi:10.1038/nclimate1783.

Peterson, T. C., and Coauthors, 2008: Why weather and climate extremes matter. *Weather and Climate Extremes in a Changing Climate. Regions of Focus: North America, Hawaii, Caribbean, and U.S. Pacific Islands*. T. R. Karl et al., Eds., U.S. Climate Change Science Program and the Subcommittee on Global Change Research, 11–33.

Petoukhov, V., and V. Semenov, 2010: A link between reduced Barents-Kara sea ice and cold winter extremes over northern continents. *J. Geophys. Res.*, **115**, D21111, doi:10.1029/2009JD013568.

——, S. Rahmstorf, S. Petri, and H. J. Schellnhuber, 2013: Quasiresonant amplification of planetary waves and recent Northern Hemisphere weather extremes. *Proc. Natl. Acad. Sci. USA*, **110**, 5336–5341.

Pierce, D. W., 2002: The role of sea surface temperatures in interactions between ENSO and the North Pacific oscillation. *J. Climate*, **15**, 1295–1308.

Pinto, J. G., N. Bellenbaum, M. K. Karremann, and P. M. Della-Marta, 2013: Serial clustering of extratropical cyclones over the North Atlantic and Europe under recent and future climate conditions. *J. Geophys. Res. Atmos.*, **118**, 12476–12485, doi:10.1002/2013JD020564.

Polade, S. D., A. Gershunov, D. R. Cayan, M. D. Dettinger, and D. W. Pierce, 2013: Natural climate variability and teleconnections to precipitation over the Pacific-North American region in CMIP3 and CMIP5 models. *Geophys. Res. Lett.*, **40**, 2296–2301.

——, D. W. Pierce, D. R. Cayan, A. Gershunov, and M. D. Dettinger, 2014: The key role of dry days in changing regional climate and precipitation regimes. *Sci. Rep.*, **4**, 4364, doi:10.1038/srep04364.

Pope, V. D., M. L. Gallani, P. R. Rowntree, and R. A. Stratton, 2000: The impact of new physical parametrizations in the Hadley Centre climate model: HadAM3. *Climate Dyn.*, **16**, 123–146, doi:10.1007/s003820050009.

Porteous, A., and B. Mullan, 2013: The 2012-13 drought: An assessment and historical perspective. MPI Tech. Paper No. 2012/18. Ministry for Primary Industries/National Institute of Water & Atmospheric Research, 57 pp. [Available online at http://www.niwa.co.nz/sites/niwa.co.nz/files/2013-18-The%202012-13%20drought%20an%20assessment%20and%20historical%20perspective.pdf.]

Power, S., T. Casey, C. Folland, A. Colman, and V. Mehta, 1999: Inter-decadal modulation of the impact of ENSO on Australia. *Climate Dyn.*, **15**, 319–324.

——, M. Haylock, R. Colman, and X. Wang, 2006: The predictability of interdecadal changes in ENSO activity and ENSO teleconnections. *J. Climate*, **19**, 4755–4771.

Prakash, S., 2013: Brief Report on visit to Alaknanda Valley, Uttarakhand Himalaya during 22-24 June 2013. [India] National Institute of Disaster Management, [12 pp.] [Available online at http://www.nidm.gov.in/pdf/Uttarakhand%20Disaster.pdf.]

PRISM, 2014: PRISM climate data. PRISM Climate Group, Oregon State University, Corvallis, OR, digital media, retrieved 10 Feb 2014. [Available online at http://prism.oregonstate.edu.]

Qian, C., and T. Zhou, 2014: Multidecadal variability of North China aridity and its relationship to PDO during 1900-2010. *J. Climate*, **27**, 1210–1222.

Qian, Y., L. Leung, S. Ghan, and F. Giorgi, 2003: Regional climate effects of aerosols over China: Modeling and observation. *Tellus*, **55B**, 914–934.

——, D. Gong, J. Fan, L. Leung, R. Bennartz, D. Chen, and W. Wang, 2009: Heavy pollution suppresses light rain in China: Observations and modeling. *J. Geophys. Res.*, **114**, D00K02, doi:10.1029/2008JD011575.

Rajeevan, M., S. Gadgil, and J. Bhate, 2010: Active and break spells of the Indian summer monsoon. *J. Earth Sys. Sci.*, **119**, 229–247.

Rayner, N. A., D. E. Parker, E. B. Horton, C. K. Folland, L. V. Alexander, D. P. Rowell, E. C. Kent, and A. Kaplan, 2003: Global analyses of sea surface temperature, sea ice, and night marine air temperature since the late nineteenth century. J. *Geophys. Res.*, **108** (D14), 4407, doi:10.1029/2002JD002670.

Rienecker, M. M., and Coauthors, 2008: The GEOS-5 data assimilation system—Documentation of versions 5.0.1, 5.1.0, and 5.2.0. NASA Tech. Rep. Series on Global Modeling and Data Assimilation, NASA/TM-2007-104606, Vol. 27, 95 pp.

——, and Coauthors, 2011: MERRA: NASA's Modern-Era Retrospective Analysis for Research and Applications. *J. Climate*, **24**, 3624–3648.

Rupp, D. E., P. W. Mote, N. Massey, C. J. Rye, R. Jones, and M. R. Allen, 2012: Did human influence on climate make the 2011 Texas drought more probable? [in "Explaining Extreme Events of 2011 from a Climate Perspective"]. *Bull. Amer. Meteor. Soc.*, **93**, 1052–1067.

——, ——, ——, F. E. L. Otto, and M. R. Allen, 2013: Human influence on the probability of low precipitation in the Central United States in 2012 [in "Explaining Extreme Events of 2012 from a Climate Perspective"]. *Bull. Amer. Meteor. Soc.*, **94** (9), S2–S6.

Sampe, T., H. Nakamura, A. Goto, and W. Ohfuchi, 2010: Significance of a midlatitude SST frontal zone in the formation of a storm track and an eddy-driven westerly jet. *J. Climate*, **23**, 1793–1814.

Schaer, C., P. L. Vidale, D. Luethi, C. Frei, C. Haeberli, M. A. Liniger, and C. Appenzeller, 2004: The role of increasing temperature variability in European summer heatwaves. *Nature*, **427**, 332–336.

Schmidt, H., and H. von Storch, 1993: German Bight storms analysed. *Nature*, **365**, 791–791.

Schneider, U., A. Becker, P. Finger, A. Meyer-Christoffer, M. Ziese, and B. Rudolf, 2014: GPCC's new land surface precipitation climatology based on quality-controlled in situ data and its role in quantifying the global water cycle. *Theor. Appl. Climatol.*, **115**, 15–40, doi:10.1007/s00704-013-0860-x.

Schubert, S., and Coauthors, 2009: A U.S. CLIVAR project to assess and compare the responses of global climate models to drought-related SST forcing patterns: Overview and results. *J. Climate*, **22**, 5251–5272.

——, H. Wang, R. Koster, M. Suarez, and P. Groisman, 2014: Northern Eurasian heat waves and droughts. *J. Climate,* **27**, 3169–3207.

Schwartz, R. M., and T. W. Schmidlin, 2002: Climatology of blizzards in the conterminous United States, 1959-2000. *J. Climate*, **15**, 1765–1772.

Screen, J. A., I. Simmonds, C. Deser, and R. Tomas, 2013: The atmospheric response to three decades of observed Arctic sea ice loss. *J. Climate*, **26**, 1230–1248.

Seneviratne, S. I., 2012: Climate science: Historical drought trends revisited. *Nature*, **491**, 338–339.

——, T. Corti, E. L. Davin, M. Hirschi, E. B. Jaeger, I. Lehner, B. Orlowsky, and A. J. Teuling, 2010: Investigating soil moisture-climate interactions in a changing climate: A review. *Earth-Sci. Rev.*, **99**, 125–161.

——, M. G. Donat, B. Mueller, and L. V. Alexander, 2014: No pause in the increase of hot temperature extremes. *Nature Climate Change*, **4**, 161–163, doi:10.1038/nclimate2145.

Sewall, J. O., 2005: Precipitation shifts over western North America as a result of declining Arctic sea ice cover: The coupled system response. *Earth Interact.*, **9**, 1–23, doi:10.1175/EI171.1.

Sheffield, J., E. F. Wood, and M. L. Roderick, 2012: Little change in global drought over the past 60 years. *Nature*, **491**, 435–438.

——, and Coauthors, 2013: North American climate in CMIP5 experiments. Part I: Evaluation of historical simulations of continental and regional climatology. *J. Climate*, **26**, 9209–9245.

Sherwood, S., and Q. Fu, 2014: A drier future? *Science*, **343**, 737–738.

Shiogama, H., M. Watanabe, Y. Imada, M. Mori, M. Ishii, and M. Kimoto, 2013: An event attribution of the 2010 drought in the south Amazon region using the MIROC5 model. *Atmos. Sci. Lett.*, **14**, 170–175.

Siderius, C., and Coauthors, 2013: Snowmelt contributions to discharge of the Ganges. *Sci. Total Environ.*, **468–469** (Suppl.), S93–S101, doi:10.1016/j.scitotenv.2013.05.084.

Sillmann, J., V. V. Kaharin, F. W. Zwiers, X. Zhang, and D. Bronaugh, 2013: Climate extreme indicies in the CMIP5 multimodel ensemble: Part 2. Future climate projections. *J. Geophys. Res. Atmos.*, **118**, 2473–2493, doi:10.1002/jgrd.50188.

——, M. G. Donat, J. C. Fyfe, and F. W. Zwiers, 2014: Observed and simulated temperature extremes during the recent warming hiatus. *Environ. Res. Lett.*, **9**, 064023, doi:10.1088/1748-9326/9/6/064023.

Singh, D., M. Tsiang, B. Rajaratnam, and N. S. Diffenbaugh, 2014: Observed changes in extreme wet and dry spells during the South Asian summer monsoon season. *Nature Climate Change*, **4**, 456–461.

Slingo, J., 2013: Why was the start to spring 2013 so cold? Met Office briefing note, April 2013. [Available online at http://www.metoffice.gov.uk/research/news/cold-spring-2013.]

Smith, T. M., R. W. Reynolds, T. C. Peterson, and J. Lawrimore, 2008: Improvements to NOAA's historical merged land-ocean surface temperature analysis (1880-2006). *J. Climate*, **21**, 2283–2296.

Solomon, A., and M. Newman, 2012: Reconciling disparate twentieth-century Indo-Pacific Ocean temperature trends in the instrumental record. *Nature Climate Change*, **2**, 691–699.

Song, F., T. Zhou, and Y. Qian, 2014: Responses of East Asian summer monsoon to natural and anthropogenic forcings in the 17 latest CMIP5 models. *Geophys. Res. Lett.*, **41**, 596–603, doi:10.1002/2013GL058705.

Sperber, K. R., H. Annamalai, I.-S. Kang, A. Kitoh, A. Moise, A. Turner, B. Wang, and T. Zhou, 2013: The Asian summer monsoon: An intercomparison of CMIP5 vs. CMIP3 simulations of the late 20th century. *Climate Dyn.*, **41**, 2711–2744.

Stark, J. D., C. J. Donlon, M. J. Martin, and M. E. McCulloch, 2007: OSTIA: An operational, high resolution, real time, global sea surface temperature analysis system. *Oceans 2007 - Europe*, Aberdeen, Scotland, IEEE, Vols. 1–3, 331–334, doi:10.1109/OCEANSE.2007.4302251.

Stocker, T. F., and Coauthors, Eds., 2014: *Climate Change 2013: The Physical Science Basis*. Cambridge University Press, 1535 pp.

Stone, D. A., and M. R. Allen, 2005: Attribution of global surface warming without dynamical models. *Geophys. Res. Lett.*, **32**, L18711, doi:10.1029/2005GL023682.

——, ——, P. A. Stott, P. Pall, S.-K. Min, T. Nozawa, and S. Yukimoto, 2009: The detection and attribution of human influence on climate. *Ann. Rev. Environ. Res.*, **34**, 1–16.

Stott, P. A., D. A. Stone, and M. R. Allen, 2004: Human contribution to the European heatwave of 2003. *Nature*, **432**, 610–614, doi:10.1038/nature03089.

Sutton, R. T., and B.-W. Dong, 2012: Atlantic Ocean influence on a shift in European climate in the 1990s. *Nature Geosci.*, **5**, 788–792, doi:10.1038/ngeo1595.

——, and P. P. Mathieu, 2002: Response of the atmosphere–ocean mixed-layer system to anomalous ocean heat-flux convergence. *Quart. J. Roy. Meteor. Soc.*, **128**, 1259–1275.

Swart, N. C., and J. C. Fyfe, 2012: Observed and simulated changes in the Southern Hemisphere surface westerly wind-stress. *Geophys. Res. Lett.*, **39**, L16711, doi:10/1029/2012GL052810.

Tait, A., R. Henderson, R. Turner, and X. Zheng, 2006: Thin plate smoothing spline interpolation of daily rainfall for New Zealand using a climatological rainfall surface. *Int. J. Climatol.*, **26**, 2097–2115.

Taylor, K. E., R. J. Stouffer, and G. A. Meehl, 2012: An overview of CMIP5 and the experiment design. *Bull. Amer. Meteor. Soc.,* **93**, 485–498.

Thompson, D. W. J., S. Solomon, P. J. Kushner, M. H. England, K. M. Grise, and D. J. Karoly, 2011: Signatures of the Antarctic ozone hole in Southern Hemisphere surface climate change. *Nature Geosci.*, **4**, 741–749, doi:10.1038/ngeo1296.

Trenberth, K. E., 2011: Changes in precipitation with climate change. *Climate Res.*, **47**, 123–138.

——, G. Branstator, and P. Arkin, 1988: Origins of the 1988 American drought. *Science*, **242**, 1640–1645.

——, A. Dai, G. van der Schrier, P. D. Jones, J. Barichivich, K. R. Briffa, and J. Sheffield, 2014: Global warming and changes in drought. *Nature Climate Change*, **4**, 17–22.

Trewin, B., 2012: A daily homogenized temperature data set for Australia. *Int. J. Climatol.*, **33**, 1510–1529, doi:10.1002/joc.3530.

Trigo, R. M., and Coauthors, 2013: The record winter drought of 2011-12 in the Iberian Peninsula [in "Explaining Extreme Events of 2012 from a Climate Perspective"]. *Bull. Amer. Meteor. Soc.*, **94** (9), S41–S45.

Uccellini, L. W., and P. J. Kocin, 1987: The interaction of jet streak circulations during heavy snow events along the East Coast of the United States. *Wea. Forecasting*, **2**, 289–308.

Ullah, K., and G. Shouting, 2013: A diagnostic study of convective environment leading to heavy rainfall during the summer monsoon 2010 over Pakistan. *Atmos. Res.*, **120–121**, 226–239.

USBR, 2014: Reclamation announces initial 2014 Central Valley Project water supply allocation. United States Bureau of Reclamation, news release, 21 February 2014. [Available online at http://www.usbr.gov/newsroom/newsrelease/detail.cfm?RecordID=46045.]

USDA, 2014a: Obama Administration announces additional assistance to Californians impacted by drought. United States Department of Agriculture, news release, 0022.14. [Available online at http://www.usda.gov/wps/portal/usda/usdamediafb?contentid=2014/02/0022.xml&printable=true&contentidonly=true.]

——, 2014b: Secretarial Disaster Designations - 2014 Crop Year. All Crop - Total Counties by State (updated 9/3/2014). United States Department of Agriculture. [Available online at http://www.usda.gov/documents/2014-all-crop-list-counties.pdf.]

USGS, cited 2014: California Water Science Center. [Available online at http://ca.water.usgs.gov/data/drought/drought-impact.html.]

van Haren, R., G. J. van Oldenborgh, G. Lenderink, and W. Hazeleger, 2013a: Evaluation of modeled changes in extreme precipitation in Europe and the Rhine basin. *Environ. Res. Lett.*, **8**, 014053, doi:10.1088/1748-9326/8/1/014053.

——, ——, ——, M. Collins, and W. Hazeleger, 2013b: SST and circulation trend biases cause an underestimation of European precipitation trends. *Climate Dyn.*, **40**, 1–20.

van Oldenborgh, G. J., A. van Urk, and M. Allen, 2012: The absence of a role of climate change in the 2011 Thailand floods. *Bull. Amer. Meteor. Soc.*, **93**, 1047–1049.

——, F. J. Doublas Reyes, S. S. Dirjfhout, and E. Hawkins, 2013: Reliability of regional climate model trends. *Environ. Res. Lett.*, **8**, 014055, doi:10.1088/1748-9326/8/1/014055.

Vautard, R., and P. Yiou, 2009: Control of recent European surface climate change by atmospheric flow. *Geophys. Res. Lett.*, **36**, L22702, doi:10.1029/2009GL040480.

——, and Coauthors, 2007: Summertime European heat and drought waves induced by wintertime Mediterranean rainfall deficit. *Geophys. Res. Lett.*, **34**, L07711, doi:10.1029/2006GL028001.

VegDRI, cited 2014: Vegetation drought response index. [Available online at http://vegdri.unl.edu/.]

Vicente-Serrano, S. M., R. M. Trigo, J. I. López-Moreno, M. L. R. Liberato, J. Lorenzo-LaCruz, S. Beguería, E. Morán-Tejada, and A. El Kenawy, 2011: Extreme winter precipitation in the Iberian Peninsula in 2010: Anomalies, driving mechanisms and future projections. *Climate Res.*, **46**, 51–65.

Visbeck, M. H., J. W. Hurrell, L. Polvani, and H. M. Cullen, 2001: The North Atlantic Oscillation: Past, present, and future. *Proc. Natl. Acad. Sci. USA*, **98**, 12876–12877.

Vose, R. S., R. L. Schmoyer, P. M. Steurer, T. C. Peterson, R. Heim, T. R. Karl, and J. K. Eischeid, 1992: The Global Historical Climatology Network: Long-term monthly temperature, precipitation, sea level pressure, and station pressure data. ORNL/CDIAC-53, NCDP-041, 325 pp.

——, and Coauthors, 2014: Improved historical temperature and precipitation time series for U.S. climate divisions. *J. App. Meteor. Climatol.*, **53**, 1232–1251.

Wakabayashi, S., and R. Kawamura, 2004: Extraction of major teleconnection patterns possibly associated with the anomalous summer climate in Japan. *J. Meteor. Soc. Japan*, **82**, 1577–1588.

Wallace, J. M., I. M. Held, D. W. J. Thompson, K. E. Trenberth, and J. E. Walsh, 2014: Global warming and winter weather. *Science*, **343**, 729–730, doi:10.1126/science.343.6172.729.

Wang, B., B. Xiang, and J.-Y. Lee, 2013: Subtropical high predictability establishes a promising way for monsoon and tropical storm predictions. *Proc. Natl. Acad. Sci. USA*, **110**, 2718–2722.

Wang, S.-Y., R. E. Davies, W.-R. Huang, and R. R. Gillies, 2011: Pakistan's two-stage monsoon and links with the recent climate change. *J. Geophys. Res.*, **116**, D16114, doi:10.1029/2011JD015760.

——, L. Hipps, R. R. Gillies, and J.-H. Yoon, 2014: Probable causes of the abnormal ridge accompanying the 2013–2014 California drought: ENSO precursor and anthropogenic warming footprint. *Geophys. Res. Lett.*, **41**, 3220–3226, doi:10.1002/2014GL059748.

Watanabe, M., and Coauthors, 2010: Improved climate simulation by MIROC5: Mean states, variability, and climate sensitivity. *J. Climate*, **23**, 6312–6335.

Water CA, cited 2014: California Department of Water Resources. [Available online at http://www.water.ca.gov/waterconditions/.]

Webster, P. J., V. O. Magaña, T. N. Palmer, J. Shukla, R. A. Tomas, M. Yanai, and T. Yasunari, 1998: Monsoons: Processes, predictability, and the prospects for prediction. *J. Geophys. Res.*, **103** (C7), 14451–14510, doi:10.1029/97JC02719.

——, V. E. Toma, and H.-M. Kim, 2011: Were the 2010 Pakistan floods predictable? *Geophys. Res. Lett.*, **38**, L04806, doi:10.1029/2010GL046346.

Weisse, R., H. von Storch, and F. Feser, 2005: Northeast Atlantic and North Sea storminess as simulated by a regional climate model during 1958-2001 and comparison with observations. *J. Climate*, **18**, 465–479.

Wen, Q. H., X. Zhang, Y. Xu, and B. Wang, 2013: Detecting human influence on extreme temperatures in China. *Geophys. Res. Lett.*, **40**, 1171–1176, doi:10.1002/grl.50285.

Westra, S., L. V. Alexander, and F. W. Zwiers, 2013: Global increasing trends in annual maximum daily precipitation. *J. Climate*, **26**, 3904–3918.

Wheeler, M. C., and H. H. Hendon, 2004: An all season real-time multivariate MJO index: Development of an index for monitoring and prediction. *Mon. Wea. Rev.*, **132**, 1917–1932.

Wilks, D. S. 2006: *Statistical Methods in the Atmospheric Sciences*. International Geophysics Series, Vol. 91, Elsevier Academic Press, 627 pp.

WMO, 2010: Guide to meteorological instruments and methods of observation. WMO No. 8. World Meteorological Society, 437 pp. [Available online at http://www.wmo.int/pages/prog/www/IMOP/CIMO-Guide.html.]

——, 2013: The state of greenhouse gases in the atmosphere based on global observations through 2012. *WMO Greenhouse Gas Bulletin*, No. 9, 4 pp.

Wu, G., Y. Liu, B. He, Q. Bao, A. Duan, and F.-F. Jin, 2012: Thermal controls on the Asian summer monsoon. *Sci. Rep.*, **2**, Article 404, doi:10.1038/srep00404.

Wu, L., and Coauthors, 2012: Enhanced warming over the global subtropical western boundary currents. *Nature Climate Change*, **29**, 161–166.

Xavier, P. K., C. Marzin, and B. N. Goswami, 2007: An objective definition of the Indian summer monsoon season and a new perspective on the ENSO–monsoon relationship. *Quart. J. Roy. Meteor. Soc.,* **133**, 749–764.

Yiou, P., and J. Cattiaux, 2013: Contribution of atmospheric circulation to wet north European summer precipitation of 2012[in "Explaining Extreme Events of 2012 from a Climate Perspective"]. *Bull. Amer. Meteor. Soc.*, **94** (9), S39–S41.

——, R. Vautard, P. Naveau, and C. Cassou, 2007: Inconsistency between atmospheric dynamics and temperatures during the exceptional 2006/2007 fall/winter and recent warming in Europe. *Geophys. Res. Lett.*, **34**, L21808, doi:10.1029/2007GL031981.

——, K. Goubanova, Z. X. Li, and M. Nogaj, 2008: Weather regime dependence of extreme value statistics for summer temperature and precipitation. *Nonlin. Processes Geophys.*, **15**, 365–378, doi:10.5194/npg-15-365-2008.

Yu, R., and T. Zhou, 2007: Seasonality and three-dimensional structure of the interdecadal change in East Asian monsoon. *J. Climate*, **20**, 5344–5355.

——, B. Wang, and T. Zhou, 2004: Tropospheric cooling and summer monsoon weakening trend over East Asia. *Geophys. Res. Lett.*, **31**, L22212, doi:10.1029/2004GL021270.

Zhang, X., F. W. Zwiers, G. C. Hegerl, F. H. Lambert, N. P. Gillett, S. Solomon, P. A. Stott, and T. Nozawa, 2007: Detection of human influence on twentieth-century precipitation trends. *Nature*, **448**, 461–465.

——, H. Wan, F. W. Zwiers, G. C. Hegerl, and S.-K. Min, 2013: Attributing intensification of precipitation extremes to human influence. *Geophys. Res. Lett.*, **40**, 5252–5257, doi:10.1002/grl.51010.

Zhou, T., D. Gong, J. Li, and B. Li, 2009: Detecting and understanding the multi-decadal variability of the East Asian Summer Monsoon - Recent progress and state of affairs. *Meteor. Z.*, **18**, 455–467.

——, F. Song, R. Lin, X. Chen, and X. Chen, 2013: The 2012 North China floods: Explaining an extreme rainfall event in the context of a long-term drying tendency [in "Explaining Extreme Events of 2012 from a Climate Perspective"]. *Bull. Amer. Meteor. Soc.*, **94** (9), S49–S51.

Zolina, O., C. Simmer, A. Kapala, P. Shabanov, P. Becker, H. Mächel, S. Gulev, and P. Groisman, 2013: New view on precipitation variability and extremes in Central Europe from a German high resolution daily precipitation dataset: Results from STAMMEX project *Bull. Amer. Meteor. Soc.*, **95**, 995–1002.

Zwiers, F. W., X. Zhang, and Y. Feng, 2011: Anthropogenic influence on long return period daily temperature extremes at regional scales. *J. Climate*, **24**, 881–892.

REFERENCES FOR SUPPLEMENTAL MATERIAL

Adler, R. F., and Coauthors, 2003: The Version 2 Global Precipitation Climatology Project (GPCP) monthly precipitation analysis (1979-Present). *J. Hydrometeor.*, **4**, 1147–1167.

Becker, A., P. Finger, A. Meyer-Christoffer, B. Rudolf, K. Schamm, U. Schneider, and M. Ziese, 2013: A description of the global land-surface precipitation data products of the Global Precipitation Climatology Centre with sample applications including centennial (trend) analysis from 1901 to present. *Earth Syst. Sci. Data,* **5**, 71–99.

Benjamini, Y., and Y. Hochberg, 1995: Controlling the false discovery rate: A practical and powerful approach to multiple testing. *J. Roy. Stat. Soc.*, **B57**, 289–300.

Bindoff, N. L., and Coauthors, 2013: Detection and attribution of climate change: From global to regional. *Climate Change 2013: The Physical Science Basis*, T. F. Stocker et al., Eds., Cambridge University Press, 867–952.

Borah, N., A. K. Sahai, R. Chattopadhyay, S. Joseph, S. Abhilash, and B. N. Goswami, 2013: A self-organizing map–based ensemble forecast system for extended range prediction of active/break cycles of Indian summer monsoon. *J. Geophys. Res. Atmos.*, **118**, 9022–9034, doi:10.1002/jgrd.50688.

Bureau of Meteorology, 2013: Australia's warmest September on record. Bureau of Meteorology Special Climate Statement 46, 26 pp. [Available online at http://www.bom.gov.au/climate/current/statements/scs46.pdf.]

Cassou, C., 2008: Intraseasonal interaction between the Madden–Julian Oscillation and the North Atlantic Oscillation. *Nature*, **455**, 523–527.

Chattopadhyay, R., A. K. Sahai, and B. N. Goswami, 2008: Objective identification of nonlinear convectively coupled phases of monsoon intraseasonal oscillation: Implications for prediction. *J. Atmos. Sci.*, **65**, 1549–1569.

Chen, S., and D. Cayan, 1994: Low-frequency aspects of the large-scale circulation and West Coast United States temperature/precipitation fluctuations in a simplified general circulation model. *J. Climate*, **7**, 1668–1683.

Christiansen, B., 2013: Changes in temperature records and extremes: are they statistically significant? *J. Climate,* **26**, 7863–7875.

Christidis, N., and P. A. Stott, 2014: Change in the odds of warm years and seasons due to anthropogenic influence on the climate. *J. Climate*, **27**, 2607–2621.

—, —, A. Scaife, A. Arribas, G. S. Jones, D. Copsey, J. R. Knight, and W. J. Tennant, 2013: A new HadGEM3-A based system for attribution of weather and climate-related extreme events. *J. Climate*, **26**, 2756–2783.

Compo, G. P., and P. D. Sardeshmukh, 2010: Removing ENSO-related variations from the climate record. *J. Climate*, **23**, 1597–1978.

Dash, S. K., M. A. Kulkarni, U. C. Mohanty, and K. Prasad, 2009: Changes in the characteristics of rain events in India. *J. Geophys. Res.*, **114**, D10109, doi:10.1029/2008jd010572.

Dee, D. P., and Coauthors, 2011: The ERA-Interim reanalysis: configuration and performance of the data assimilation system. *Quart. J. Roy. Meteor. Soc.*, **137**, 553–597, doi:10.1002/qj.828.

Dong, B.-W., R. T. Sutton, and T. Woollings, 2013: The extreme European summer 2012 [in "Explaining Extreme Events of 2012 from a Climate Perspective"]. *Bull. Amer. Meteor. Soc.,* **94** (9), S28–S32.

Feldstein, S. B., 2000: The timescale, power spectra, and climate noise properties of teleconnection patterns. *J. Climate*, **13**, 4430–4440.

Flato, G., and Coauthors, 2013: Evaluation of climate models. *Climate Change 2013: The Physical Science Basis,* T. F. Stocker et al., Eds., Cambridge University Press, 741–866.

Galloway, J. M., A. Wigston, R.T. Patterson, G.T. Swindles, E. Reinhardt, H.M. Roe, 2013: Climate change and decadal to centennial-scale periodicities recorded in a late Holocene NE Pacific marine record: Examining the role of solar forcing. *Palaeogeogr., Palaeoclimatol., Palaeoecol.*, **386**, 669–689.

Ghosh, S., D. Das, S.-C. Kao, and A. R. Ganguly, 2012: Lack of uniform trends but increasing spatial variability in observed Indian rainfall extremes. *Nature Climate Change*, **2**, 86–91, doi:10.1038/nclimate1327.

Hewitson, B. C., and R. G. Crane, 2002: Self-organizing maps: Applications to synoptic climatology. *Climate Res.*, **22**, 13–26.

Hewitt, H. T., D. Copsey, I. D. Culverwell, C. M. Harris, R. S. R. Hill, A. B. Keen, A. J. McLaren, and E. C. Hunke, 2011: Design and implementation of the infrastructure of HadGEM3: the next-generation Met Office climate modelling system. *Geosci. Model Dev.*, **4**, 223–253.

Hudson, D., A. G. Marshall, Y. Yin, O. Alves and H. H. Hendon, 2013: Improving intraseasonal prediction with a new ensemble generation strategy. *Mon. Wea. Rev.*, **141**, 4429–4449.

Hurrell, J., and Coauthors, 2013: The Community Earth System Model: A framework for collaborative research. *Bull. Amer. Meteor. Soc.*, **94**, 1339–1360.

Johnson, N. C., 2013: How many ENSO flavors can we distinguish? *J. Climate*, **26**, 4816–4827.

—, S. B. Feldstein, and B. Tremblay, 2008: The continuum of Northern Hemisphere teleconnection patterns and a description of the NAO Shift with the use of self-organizing maps. *J. Climate*, **21**, 6354–6371.

Jones, D. A., W. Wang, and R. Fawcett, 2009: High-quality spatial climate data-sets for Australia. *Aust. Meteor. Ocean. J.*, **58**, 233–248.

Kalnay, E., and Coauthors, 1996: The NCEP/NCAR 40-Year Reanalysis Project. *Bull. Amer. Meteor. Soc.*, **77**, 437–471.

Knutson, T. R., F. Zeng, and A. T. Wittenberg, 2013: Multimodel assessment of regional surface temperature trends: CMIP3 and CMIP5 Twentieth Century simulations. *J. Climate*, **26**, 8709–8743.

Kohonen, T., 2001: *Self-Organizing Maps*. 3rd ed. Springer Series in Information Sciences, Vol. 30, Springer, 501 pp.

Lewis, S. C., and D. J. Karoly, 2013: Anthropogenic contributions to Australia's record summer temperatures of 2013. *Geophys. Res. Lett.*, **40**, 3705–3709, doi:10.1002/grl.50673.

Lim, E.-P., H. H. Hendon, D. L. T. Anderson, and A. Charles, 2011: Dynamical, statistical-dynamical, and multimodel ensemble forecasts of Australian spring season rainfall. *Mon. Wea. Rev.,* **139**, 958–975.

Liu, Y., R. H. Weisberg, and C. N. K. Mooers, 2006: Performance evaluation of the self-organizing map for feature extraction. *J. Geophys. Res.*, **111**, C05018, doi:10.1029/2011GL047658.

Livezey, R. E., and W. Y. Chen, 1983: Statistical field significance and its determination with Monte Carlo techniques. *Mon. Wea. Rev.*, **111**, 46–59.

Mastrandrea, M. D., K. J. Mach, G.-K. Plattner, O. Edenhofer, T. F. Stocker, C. B. Field, K. L. Ebi, and P. R. Matschoss, 2011: The IPCC AR5 guidance note on consistent treatment of uncertainties: A common approach across the working groups. *Climatic Change*, **108**, 675–691.

Mitchell, T., and W. Blier, 1997: The variability of wintertime precipitation in the region of California. *J. Climate*, **10,** 2261–2276.

Mo, R., and D. M. Straus, 2002: Statistical–dynamical seasonal prediction based on principal component regression of GCM ensemble integrations. *Mon. Wea. Rev.*, **130**, 2167–2187.

Morice, C. P., J. J. Kennedy, N. A. Rayner, and P. D. Jones, 2012: Quantifying uncertainties in global and regional temperature change using an ensemble of observational estimates: The HadCRUT4 dataset. *J. Geophys. Res.*, **117**, D08101, doi:10.1029/2011JD017187.

Moss, R. H., and Coauthors, 2010: The next generation of scenarios for climate change research and assessment. *Nature*, **463**, 747–756.

Murphy, J. M., D. M. H. Sexton, D. N. Barnett, G. S. Jones, M. J. Webb, M. Collins, and D. A. Stainforth, 2004: Quantification of modelling uncertainties in a large ensemble of climate change simulations. *Nature*, **430**, 768–772.

Pall, P., T. Aina, D. A. Stone, P. A. Stott, T. Nozawa, A. G. J. Hilberts, D. Lohmann, and M. R. Allen, 2011: Anthropogenic greenhouse gas contribution to flood risk in England and Wales in autumn 2000. *Nature*, **470**, 382–385.

Park, S., and C. S. Bretherton, 2009: The University of Washington shallow convection and moist turbulence schemes and their impact on climate simulations with the Community Atmosphere Model. *J. Climate*, **22**, 3449–3469.

Polade, S. D., A. Gershunov, D. R. Cayan, M. D. Dettinger and D. W. Pierce, 2013: Natural climate variability and teleconnections to precipitation over the Pacific-North American region in CMIP3 and CMIP5 models. *Geophys. Res. Lett.*, **40**, 2296–2301, doi:10.1002/grl.50491.

Porteous, A., and B. Mullan, 2013: The 2012-13 drought: An assessment and historical perspective. MPI Tech. Paper No. 2012/18, Ministry for Primary Industries/National Institute of Water & Atmospheric Research, 57 pp. [Available online at http://www.niwa.co.nz/sites/niwa.co.nz/files/2013-18-The%202012-13%20drought%20an%20assessment%20and%20historical%20perspective.pdf.]

Rajeevan, M., J. Bhate, J. Kale, and B. Lal, 2006: A high resolution daily gridded rainfall for the Indian region: Analysis of break and active monsoon spells. *Current Sci.*, **91**, 296–306.

—, S. Gadgil, and J. Bhate, 2010: Active and break spells of the Indian summer monsoon. *J. Earth Sys. Sci.*, **119**, 229–247, doi:10.1007/s12040-010-0019-4.

Raupach, M. R., P. R. Briggs, V. Haverd, E. A. King, M. Paget, and C. M. Trudinger, 2009: Australian Water Availability Project (AWAP): CSIRO Marine and Atmospheric Research Component: Final Report for Phase 3. CAWCR Technical Report No.013, 67 pp.

Reusch, D. B., R. B. Alley, and B. C. Hewitson, 2005: Relative performance of self-organizing maps and principal component analysis in pattern extraction from synthetic climatological data. *Polar Geogr.*, **29**, 188–212.

Reynolds, R. W., N. A. Rayner, T. M. Smith, D. C. Stokes, and W. Wang, 2002: An improved in situ and satellite SST analysis for climate. *J. Climate*, **15**, 1609–1625.

Saji, N. H., B. N. Goswami, P. N. Vinayachandran, and T. Yamagata, 1999: A dipole mode in the tropical Indian Ocean. *Nature*, **401**, 360–363.

Shin, S., and P. D. Sardeshmukh, 2011: Critical influence of the pattern of tropical ocean warming on remote climate trends. *Climate Dyn.*, **36**, 1577–1591.

Singh, C., 2013: Characteristics of monsoon breaks and intraseasonal oscillations over central India during the last half century. *Atmos. Res.*, **128**,120–128, doi:10.1016/j.atmosres.2013.03.003.

Slingo, J., 2013: Why was the start to spring 2013 so cold? Met Office briefing note, April 2013. [Available online at http://www.metoffice.gov.uk/research/news/cold-spring-2013.]

Smith, T. M., R. W. Reynolds, T. C. Peterson, and J. Lawrimore, 2008: Improvements to NOAA's Historical Merged Land-Ocean Surface Temperature analysis (1880-2006). *J. Climate*, **21**, 2283–2296.

Solomon, A., and M. Newman, 2012: Reconciling disparate twentieth-century Indo-Pacific ocean temperature trends in the instrumental record. *Nature Climate Change*, **2**, 691–699.

Sperber, K. R., H. Annamalai, I.-S. Kang, A. Kitoh, A. Moise, A. Turner, B. Wang, and T. Zhou, 2013: The Asian summer monsoon: An intercomparison of CMIP5 vs. CMIP3 simulations of the late 20th century. *Climate Dyn.*, **41**, 2711–2744.

Stark, J. D., C. J. Donlon, M. J. Martin, and M. E. McCulloch, 2007: OSTIA: An operational, high resolution, real time, global sea surface temperature analysis system. *Oceans 2007 - Europe*, Aberdeen, Scotland, IEEE, Vols. 1–3, 331–334, doi:10.1109/OCEANSE.2007.4302251.

Stott, P. A., G. S. Jones, J. A. Lowe, P. Thorne, C. F. Durman, T. C. Johns, and J.-C. Thelen, 2006: Transient climate simulations with the HadGEM1 climate model: Cases of past warming and future climate change. *J. Climate*, **19**, 2763–2782.

Taylor, K. E., R. J. Stouffer, and G. A. Meehl, 2012: An overview of CMIP5 and the experiment design. *Bull. Amer. Meteor. Soc.*, **93**, 485–498.

Tennant, W. J., G. J. Shutts, A. Arribas, and S. A. Thompson, 2011: Using a stochastic kinetic energy backscatter scheme to improve MOGREPS probabilistic forecast skill. *Mon. Wea. Rev.*, **139**, 1190–1206.

White, C. J., D. Hudson, and O. Alves, 2014: ENSO, the IOD and the intraseasonal prediction of heat extremes across Australia using POAMA-2. *Climate Dyn.*, doi:10.1007/s00382-013-2007-2.

Wilks, D. S., 2006: On "field significance" and the false discovery rate. *J. Appl. Meteor. Climatol.*, **45**, 1181–1189.

Zanchettin, D., A. Rubino, and J. H. Jungclaus, 2010: Intermittent multidecadal-to-centennial fluctuations dominate global temperature evolution over the last millennium. *Geophys. Res. Lett.*, **37**, L14702, doi:10.1029/2010GL043717.

Zhang, G. J., and N. A. McFarlane, 1995: Sensitivity of climate simulations to the parameterization of cumulus convection in the Canadian Climate Centre general circulation model. *Atmos.—Ocean*, **33**, 407–446.